Annu. Rev. Fluid Mech. 1997. 29:27–64

ELECTROHYDRODYNAMICS: The Taylor-Melcher Leaky Dielectric Model

D. A. Saville
Department of Chemical Engineering, Princeton University Princeton, New Jersey 08544

KEY WORDS: electrified drops and jets, suspensions, interface charge, bulk charge

ABSTRACT

Electrohydrodynamics deals with fluid motion induced by electric fields. In the mid 1960s GI Taylor introduced the leaky dielectric model to explain the behavior of droplets deformed by a steady field, and JR Melcher used it extensively to develop electrohydrodynamics. This review deals with the foundations of the leaky dielectric model and experimental tests designed to probe its usefulness. Although the early experimental studies supported the qualitative features of the model, quantitative agreement was poor. Recent studies are in better agreement with the theory. Even though the model was originally intended to deal with sharp interfaces, contemporary studies with suspensions also agree with the theory. Clearly the leaky dielectric model is more general than originally envisioned.

INTRODUCTION

The earliest record of an electrohydrodynamic experiment is in William Gilbert's seventeenth century treatise *de Magnete*, which describes the formation of a conical shape upon bringing a charged rod above a sessile drop (Taylor 1969). Nineteenth-century studies of drop dynamics revealed how radially directed forces stemming from interfacial charge offset surface tension (Rayleigh 1882), but until the 1960s most work focused on the behavior of *perfect conductors*, (mercury or water) or *perfect dielectrics* (apolar liquids such as benzene). This began to change following studies on poorly conducting liquids—*leaky dielectrics*—by Allan & Mason (1962). Another branch of electrohydrodynamics, electrokinetics, deals with the behavior of charged particles in aqueous electrolytes (Saville 1977, Russel et al 1989). However, there are significant differences between the behavior of electrolytes and leaky dielectrics. In electrolytes, electrokinetic phenomena are dominated by effects of interface

0066-4189/97/0115-0027$08.00

charge derived from covalently bound ionizable groups or ion adsorption. Near a surface charged in this fashion, a diffuse charge cloud forms as electrolyte ions of opposite charge are attracted toward the interface. A concentration gradient forms so that diffusion balances electromigration. Then, when a field is imposed, processes in this diffuse layer govern the mechanics. In electrokinetics, applied field strengths are small, a few volts per centimeter, whereas in electrohydrodynamics the fields are usually much larger. With perfect conductors, perfect dielectrics, or leaky dielectrics, diffuse layers associated with equilibrium charge are usually absent. Accordingly, development of the two subjects proceeded more or less independently. Nevertheless, the underlying processes share many characteristics. Most obvious is that electric charge and current originate with ions; therefore, charge may be induced in poorly conducting liquids even though equilibrium charge is absent. The different treatments began to merge with the appearance of Taylor's 1966 paper on drop deformation and Melcher & Taylor's review of the topic (1969).

Applications of electrohydrodynamics (EHD) abound: spraying, the dispersion of one liquid in another, coalescence, ink jet printing, boiling, augmentation of heat and mass transfer, fluidized bed stabilization, pumping, and polymer dispersion are but a few. Some applications of EHD are striking. For example, EHD forces have been used to simulate the earth's gravitational field during convection experiments carried out during a space shuttle flight (Hart et al 1986). In this application, combining a radial electric field with a temperature gradient between concentric spheres engenders polarization forces that mimic gravity. One of the more unusual appearances of EHD involves the blue haze found above heavily forested areas. BR Fish (1972) provides experimental evidence to support his proposition that the haze derives from waxy substances sprayed into the atmosphere from the tips of pine needles by high fields accompanying the overhead passage of electrified clouds during thunderstorms. This review concentrates on what has come to be known as the leaky dielectric model to elucidate its structure and describe its experimental foundations. For insight into other aspects of EHD, one or more of the many reviews or monographs[1] may be consulted (Arp et al 1980, Melcher 1972, 1981, Tobazeon 1984, Crowley 1986, Chang 1987, Bailey 1988, Scott 1989, Ptasinski & Kerkhof 1992, Castellanos 1994, Atten & Castellanos 1995).

In its most elementary form the leaky dielectric model consists of the Stokes equations to describe fluid motion and an expression for the conservation of current employing an Ohmic conductivity. Electromechanical coupling occurs only at fluid-fluid boundaries where charge, carried to the interface by

[1]Depending on the keywords used, computer literature surveys turn up hundreds of papers on EHD since the 1960s.

conduction, produces electric stresses different from those present in perfect dielectrics or perfect conductors. With perfect conductors or dielectrics the electric stress is perpendicular to the interface, and alterations of interface shape combined with interfacial tension serve to balance the electric stress. Leaky dielectrics are different because free charge accumulated on the interface modifies the field. Viscous flow develops to provide stresses to balance the action of the tangential components of the field acting on interface charge.

This review is organized as follows: First the model is outlined to identify approximations and potential pitfalls. Then experimental and theoretical results for two prototypical geometries—drops and cylinders—are surveyed. This discussion will establish the status of the leaky dielectric model where forces are confined to a sharp boundary. In closing, recent results on motion produced by EHD body forces are surveyed to indicate how the model has been extended to new situations.

BALANCE LAWS

The differential equations describing EHD arise from equations describing the conservation of mass and momentum, coupled with Maxwell's equations. To establish a context for the approximations inherent in the leaky dielectric model, it is necessary to look on a deeper level. Then the leaky dielectric model arises naturally through a scale analysis. As noted earlier, the hydrodynamic model consists of the Stokes equations without any electrical forces; coupling to the electric field occurs at boundaries, so forces from the bulk free charge must be negligible. Moreover, the electric field is solenoidal. The next section examines how to establish conditions under which these approximations are appropriate.

Scale Analysis and the Leaky Dielectric Model

Under static conditions, electric and magnetic phenomena are independent since their fields are uncoupled (Feynman et al 1964). Insofar as the characteristic time for electrostatic processes is large compared to that for magnetic phenomena, the electrostatic equations furnish an accurate approximation. When external magnetic fields are absent, magnetic effects can be ignored completely. From Maxwell's equations, the characteristic time for electric phenomena, $\tau_c \equiv \varepsilon\varepsilon_o/\sigma$, can be identified as the ratio of the dielectric permeability[2] ($\varepsilon\varepsilon_o$) and conductivity[3] (σ). For magnetic phenomena the characteristic time, $\tau_M \equiv \mu\mu_o\sigma\ell^2$, is the product of the magnetic permeability, $\mu\mu_o$, conductivity, and the square of a characteristic length. Transport process time-scales, τ_P, arise

[2]The rationalized Meter-Kilogram-Second-Coulomb (MKSC) system of units will be used.

[3]The conductivity will be defined explicitly in terms of properties of the constituent ions. For the present note simply that conductivity has the dimensions of Siemans per meter, i.e., C^2-s/kg-m^3.

from viscous relaxation, diffusion, oscillation of an imposed field, or motion of a boundary. Slow processes are defined as those where $\tau_P \geq \tau_C \gg \tau_M$. The second inequality can be rearranged to $(\varepsilon/\mu)^{1/2}\varepsilon_o/\sigma \gg \ell(\mu_o\varepsilon_o)^{1/2}$, and since $(\mu_o\varepsilon_o)^{-1/2}$ is equal to the speed of light, 3×10^8 m/s, $\ell(\mu_o\varepsilon_o)^{1/2}$ is very small for our systems. For the electrostatic approximation to apply on a millimeter-scale, the electrical relaxation time, $\varepsilon\varepsilon_o/\sigma$, must be longer than 10^{-12} s. The inequality is satisfied easily because the conductivity is seldom larger than one micro-Siemans per meter for liquids of the sort under study here. Accordingly, the electrical phenomena are described by

$$\nabla \cdot \varepsilon\varepsilon_o\mathbf{E} = \rho^e \tag{1}$$

and

$$\nabla \times \mathbf{E} = \mathbf{0}. \tag{2}$$

$\mathbf{E}$ is the electric field strength, and ρ^e is the local free charge density. Boundary conditions derived from Equations 1 and 2 using the divergence theorem and a pill-box system spanning a portion of a boundary show that the tangential components of $\mathbf{E}$ are continuous and the normal component jumps by an amount proportional to the free charge per unit area, q, that is,

$$\|\varepsilon\varepsilon_o\mathbf{E}\| \cdot \mathbf{n} = q. \tag{3}$$

Here $\|(\cdot)\|$ denotes the jump, "outside–inside," of $(\cdot)$ across the boundary, and $\mathbf{n}$ is the local outer normal.

Electrostatic phenomena and hydrodynamics are coupled through the Maxwell stress tensor. A simple way of seeing the relationship between Maxwell stresses and the electrical body force is to suppose that electrical forces exerted on free charge and charge dipoles are transferred directly to the fluid. For a dipole charge Q with orientation $\mathbf{d}$ the force is $(Q\mathbf{d}) \cdot \nabla\mathbf{E}$. With N dipoles per unit volume, the dipole force is $\mathbf{P} \cdot \nabla\mathbf{E}$; $\mathbf{P} \equiv N Q\mathbf{d}$ defines the polarization vector. The Coulomb force due to free charge is $\rho^e\mathbf{E}$, so the total electrical force per unit volume is $\rho^e\mathbf{E} + \mathbf{P} \cdot \nabla\mathbf{E}$. This force can be transformed into the divergence of a tensor, $\nabla \cdot [\varepsilon\varepsilon_o\mathbf{E}\mathbf{E} - \frac{1}{2}\varepsilon\varepsilon_o\mathbf{E} \cdot \mathbf{E}\boldsymbol{\delta}]$, using Equations 1 and 2. The tensor becomes the Maxwell stress tensor, $\boldsymbol{\sigma}^M$,

$$\varepsilon\varepsilon_o\mathbf{E}\mathbf{E} - \frac{1}{2}\varepsilon\varepsilon_o\left[1 - \frac{\rho}{\varepsilon}\left(\frac{\partial\varepsilon}{\partial\rho}\right)_T\right]\mathbf{E} \cdot \mathbf{E}\boldsymbol{\delta},$$

upon inserting the isotropic influence of the field on the pressure (Landau & Lifshitz 1960).

Using the expression for the electrical stress produces the equation of motion for an incompressible Newtonian fluid of uniform viscosity,

$$\rho \frac{D\mathbf{u}}{Dt} = -\nabla p + \nabla \cdot \boldsymbol{\sigma}^M + \mu \nabla^2 \mathbf{u}. \tag{4}$$

Alternatively, upon expanding the stress tensor the electrical stresses emerge as body forces due to a non-homogeneous dielectric permeability and free charge, along with the gradient of an isotropic contribution,

$$\rho \frac{D\mathbf{u}}{Dt} = -\nabla \left[p - \frac{1}{2} \varepsilon_o \rho \left(\frac{\partial \varepsilon}{\partial \rho} \right)_T \mathbf{E} \cdot \mathbf{E} \right] - \frac{1}{2} \varepsilon_o \mathbf{E} \cdot \mathbf{E} \nabla \varepsilon + \rho^e \mathbf{E} + \mu \nabla^2 \mathbf{u}. \tag{5}$$

For incompressible fluids, the expression in brackets can be lumped together as a redefined pressure.

EHD motions are driven by the electrical forces on boundaries or in the bulk. The net Maxwell stress at a sharp boundary has the normal and tangential components

$$\begin{aligned} [\boldsymbol{\sigma}^M \cdot \mathbf{n}] \cdot \mathbf{n} &= \frac{1}{2} \left\| \varepsilon \varepsilon_o (\mathbf{E} \cdot \mathbf{n})^2 - \varepsilon \varepsilon_o (\mathbf{E} \cdot \mathbf{t}_1)^2 - \varepsilon \varepsilon_o (\mathbf{E} \cdot \mathbf{t}_2)^2 \right\| \\ [\boldsymbol{\sigma}^M \cdot \mathbf{n}] \cdot \mathbf{t}_\mathbf{i} &= q \mathbf{E} \cdot \mathbf{t}_\mathbf{i} \end{aligned} \tag{6}$$

after absorbing the isotropic part of the stress into the pressure as noted above. It is understood that $\mathbf{t}_\mathbf{i}$ represents either of two orthogonal tangent vectors embedded in the surface. Denoting a characteristic field strength as E_o and balancing the tangential electrical stress in Equation 6 against viscous stress yields a velocity scale of $q\ell E_o/\mu = \varepsilon_o \ell E_o^2/\mu$. The same scale appears when the normal stress or the bulk electrical forces are used. With $\varepsilon_o E_o^2$ as a scale for pressure, Equation 5 can be cast in dimensionless form as

$$\frac{\tau_\mu}{\tau_P} \frac{\partial \mathbf{u}}{\partial t} + Re\, \mathbf{u} \cdot \nabla \mathbf{u} = -\nabla p - \frac{1}{2} \mathbf{E} \cdot \mathbf{E} \nabla \varepsilon + [\nabla \cdot (\varepsilon \mathbf{E})] \mathbf{E} + \nabla^2 \mathbf{u}. \tag{7}$$

Here the symbols represent dimensionless variables with lengths scaled by ℓ and time by the process scale τ_P; Re is a Reynolds number, $\rho \ell u_o/\mu \equiv \rho \varepsilon_o \ell^2 E_o^2/\mu^2$, when the electrohydrodynamic velocity scale is used for u_o. Choosing $\rho = 10^3$ kg/m^3, $\mu = 1$ kg/m-s, $\ell = 10^{-3}$ m, and $E_o = 10^5$ V/m gives $Re \approx 10^{-4}$ and a viscous relaxation time, $\tau_\mu \equiv \ell^2 \rho/\mu$, of 1 ms approximately. For a dielectric constant of 4 and a conductivity of 10^{-9} S/m the electrical relaxation time, $\varepsilon \varepsilon_o/\sigma$, is 35 ms.

Equation 1 shows how the field is altered by the presence of free charge. In liquids, charge is carried by ions, so species conservation equations must be

included to complete the description. Free charge density and ion concentration are related as

$$\rho^e = \sum_k ez^k n^k. \tag{8}$$

Here e is the charge on a proton and z^k is the valence of the k^{th} species whose concentration is n^k. Note that some of the species may be electrically neutral, that is, $z^k = 0$. Molecules and ions are carried by the flow and move in response to gradients in the electrochemical potential. If we denote the mobility of the k^{th} species by ω^k, the species conservation equation is

$$\frac{\partial n^k}{\partial t} + \mathbf{u}\cdot\nabla n^k = \nabla\cdot[-\omega^k ez^k n^k \mathbf{E} + \omega^k k_B T \nabla n^k] + r^k, \quad k = 1, \ldots, N. \tag{9}$$

Here k_B is Boltzmann's constant, and T is the absolute temperature. The first term on the right represents ion migration in the electric field, the second describes transport by diffusion, and the third denotes production due to chemical reactions since the neutral species act as a source for ions in the bulk. With a single ionic species, $N = 1$ and $r^1 = 0$; for a binary, z-z electrolyte, $N = 3$. In the first case, ions are produced by reactions at electrodes—this is called *unipolar injection*. With a z-z electrolyte, ions are produced at the electrodes and by homogeneous reactions within the fluid. Here attention is focused on liquids with charge from a single 1-1 electrolyte so that there are two homogeneous reactions. A forward reaction producing positive and negative ions from dissociation of the neutral species as

$$\begin{aligned}&(\text{neutral species}, k = 1, z^1 = 0)\\ &\quad \rightarrow (\text{cation}, k = 2, z^2 = 1) + (\text{anion}, k = 3, z^3 = -1)\end{aligned} \tag{10a}$$

with a rate per unit volume, $k_+ n^1$, proportional to the concentration of species 1. The recombination reaction is

$$\begin{aligned}&(\text{cation}, k = 2, z^2 = 1) + (\text{anion}, k = 3, z^3 = -1)\\ &\quad \rightarrow (\text{neutral species}, k = 1, z^1 = 0)\end{aligned} \tag{10b}$$

with a rate of $k_- n^2 n^3$. The rate constants k_+ and k_- are specific to the ions, neutral species, and solvent; the rate of production of cations or anions is $k_+ n^1 - k_- n^2 n^3$. Thus,

$$-r^1 = r^2 = r^3 = k_+ n^1 - k_- n^2 n^3 \tag{11}$$

This situation contrasts sharply with that for strong electrolytes where neutral species are dissociated fully and reaction terms absent. Because ionic reactions

are fast, it is convenient to imagine that the reactions are almost at equilibrium. At equilibrium, the local rate of reaction is zero, so $K \equiv k_+/k_- = n^2n^3/n^1$. This complicates matters because at equilibrium one of the conservation laws must be discarded to avoid an overdetermined system.

To scale the problem consistently, note that the concentrations of the two ionic species will be much smaller than the concentration of the neutral constituent. Accordingly, it is convenient to use different concentration scales. Neutral species concentrations are scaled with a bulk concentration denoted as n^0 and ionic concentrations with $\sqrt{n^0K}$. Using ω^0 as a mobility scale (any one of the three mobilities) and k_+n^0 as a reaction rate scale produces the conservation law for the neutral species,

$$\frac{\tau_D}{\tau_P}\frac{\partial n^1}{\partial t} + Pe\mathbf{u}\cdot\nabla n^1 = \omega^1\nabla^2 n^1 - Da[n^1 - n^2n^3] \tag{12a}$$

and for each ionic species,

$$\frac{\tau_D}{\tau_P}\frac{\partial n^k}{\partial t} + Pe\mathbf{u}\cdot\nabla n^k = \beta\nabla\cdot[-z^k n^k\omega^k\mathbf{E}] + \omega^k\nabla^2 n^k + Da\sqrt{\frac{n^0}{K}}[n^1 - n^2n^3], \quad k = 2\,,\ 3. \tag{12b}$$

The new symbols represent a characteristic diffusion time, $\tau_D \equiv \ell^2/\omega^0k_BT$; a Peclet number, $Pe \equiv \ell u_o/\omega^0k_BT \equiv \ell^2\varepsilon_oE_o^2/\mu\omega^0k_BT$ (the ratio of the rates of ion transfer by convection to diffusion); a dimensionless field strength, $\beta \equiv \ell eE_o/k_BT$; and a Damkoler number, $Da \equiv k_+\ell^2/\omega^0k_BT$ (the ratio of a characteristic diffusion time to a characteristic reaction time). The reaction term can be eliminated from Equation 12b using Equation 12a to obtain

$$\frac{\tau_D}{\tau_P}\frac{\partial}{\partial t}\left[n^k + \sqrt{\frac{n^0}{K}}n^1\right] + Pe\mathbf{u}\cdot\nabla\left[n^k + \sqrt{\frac{n^0}{K}}n^1\right] = \beta\nabla\cdot[-z^k n^k\omega^k\mathbf{E}] + \nabla^2\left[\omega^k n^k + \omega^1\sqrt{\frac{n^0}{K}}n^1\right], \quad k = 2, 3. \tag{12c}$$

To compute local concentrations for systems in local reaction equilibrium, Equation 12c is used with $k = 2$ and $k = 3$, along with the equation for reaction equilibrium obtained from Equation 12a for $Da \gg 1$.

Equations 12c for $k = 2$ and $k = 3$ can be combined to furnish an expression for the dimensionless charge density, $\rho^e = (n^2 - n^3)$,

$$\frac{\tau_D}{\tau_P}\frac{\partial}{\partial t}\rho^e + Pe\mathbf{u}\cdot\nabla\rho^e = \beta\nabla\cdot[-(n^2\omega^2 + n^3\omega^3)\mathbf{E}] + \nabla^2[\omega^2n^2 + \omega^3n^3]. \tag{13}$$

From Equations 1 and 13 the characteristic charge relaxation time can now be identified (in dimensional form) as $\varepsilon\varepsilon_o/e^2(\omega^2 n^2 + \omega^3 n^3) \equiv \varepsilon\varepsilon_o/\sigma$. To guide simplification of these equations, the magnitudes of the various groups are estimated for small ions with a characteristic radius[4], a, of 0.25 nm using the Stokes-Einstein relation, $(6\pi\mu a)^{-1}$, for the mobility. Then $Pe \approx 10^5$, $\beta \approx 10^3$, and the diffusion time $\tau_D \approx 10^6$ s. Estimating the size of the other dimensionless groups will require knowledge of the dissociation-recombination reactions.

The equilibrium constant, K, is estimated from the Bjerrum-Fouss theory of ion association (Fouss 1958, Moelwyn-Hughes 1965, Castellanos 1994) as in

$$K = \frac{3\pi}{4a^3} \exp\left[-\frac{e^2}{8\pi a\varepsilon\varepsilon_o k_B T}\right]. \tag{14}$$

while the recombination rate constant (Debye 1942)

$$k_- = \frac{4\pi e^2(\omega^2 + \omega^3)}{\varepsilon\varepsilon_o} \tag{15}$$

gives a forward rate constant of

$$k_+ = k_- K. \tag{16}$$

Using the data already introduced, $K \approx 10^{17}\,\mathrm{m}^{-3}$ and $k_- \approx 10^{-18}\,\mathrm{m}^3/\mathrm{s}$ so $k_+ \approx 10^{-1}$ s. Accordingly, $Da \approx 10^5$.

To estimate the concentration of charge carriers, we use an expression for the conductivity of a solution with monovalent ions derived from a single 1-1 electrolyte

$$\sigma = e^2(\omega^2 n^2 + \omega^3 n^3). \tag{17}$$

For a conductivity of 10^{-9} S/m with 0.25 nm ions, $n^2 = n^3 = 10^{20}\,\mathrm{m}^{-3}$ ($\approx 10^{-7}$ moles/liter), so $n^1 = 10^{24}\,\mathrm{m}^{-3}$ ($\approx 10^{-3}$ mol/liter). Thus, $n^0/K \approx 10^7$ and $Da\sqrt{n^0/K} \approx 10^7$. To complete the simplification we need to know the charge density.

Equation 1 in dimensionless form is

$$\Lambda\nabla \cdot \mathbf{E} = \rho^e = z(n^2 - n^3); \tag{18}$$

$\Lambda \equiv \varepsilon\varepsilon_o E_o/e\,\ell\sqrt{n^0 K}$. Using the numerical values already defined, $\Lambda \approx 10^{-4}$, suggesting the fluid is electrically neutral on the millimeter length scale. For

[4]For comparison, the radius of a sodium ion in water is 0.14 nm. The size of the charge carrying ions in apolar liquids is largely a matter of speculation, but the presence of traces of water makes it likely that the charge carriers are larger than the bare ions.

$\Lambda \ll 1$ Equation 13 yields the classical Ohm's law approximation in dimensionless form,

$$\nabla \cdot [(z)^2 n^2 (\omega^2 + \omega^3)]\mathbf{E} = 0 \tag{19}$$

as long as $Pe\Lambda/\beta \ll 1$. With the numerical magnitudes given thus far, $Pe\Lambda/\beta \approx 10^{-2}$, prompting the approximation expressed by Equation 19.

To complete the description, charge conservation at the interface must be investigated. Here it is convenient to start with Equation 9 and integrate across an interface with the provision that there are no surface reactions. Using the s-subscript to denote surface concentrations and operators, and ignoring any special transport processes such as lateral surface diffusion, leads to

$$\frac{\partial n_s^k}{\partial t} + \mathbf{u} \cdot \nabla_s n_s^k = n_s^k \mathbf{n} \cdot (\mathbf{n} \cdot \nabla)\mathbf{u} + \left\| -\omega^k e z^k n^k \mathbf{E} + \omega^k k_B T \nabla n^k \right\| \cdot \mathbf{n}. \qquad k = 2, 3. \tag{20}$$

$\nabla_s \cdot (\,)$ is the surface divergence, and n_s^k are surface concentrations. The terms on the right stand for changes in concentration due to dilation of the surface and transport to the surface by electromigration and diffusion. Adding the two equations, weighing each by the valence and the charge on a proton, gives

$$\frac{\partial q}{\partial t} + \mathbf{u} \cdot \nabla_s q = q\mathbf{n} \cdot (\mathbf{n} \cdot \nabla)\mathbf{u} + \| -e^2(\omega^2 n^2 + \omega^3 n^3)\mathbf{E} \| \cdot \mathbf{n} + \left\| k_B T \nabla (e\omega^2 n^2 - e\omega^3 n^3) \right\| \cdot \mathbf{n}. \tag{21}$$

Next Equation 21 is put in dimensionless form using $\varepsilon_o E_o$ as a surface charge scale

$$\frac{\tau_c}{\tau_P}\frac{\partial q}{\partial t} + \frac{\tau_c}{\tau_F}[\mathbf{u} \cdot \nabla_s q - q\mathbf{n} \cdot (\mathbf{n} \cdot \nabla)\mathbf{u}] = \| -(\omega^2 n^2 + \omega^3 n^3)\mathbf{E} \| \cdot \mathbf{n} + \frac{1}{\beta} \| \nabla (\omega^2 n^2 - \omega^3 n^3) \| \cdot \mathbf{n}. \tag{22}$$

A new time scale, the convective flow time $\tau_F \equiv \ell/u_F$, appears here. For $\beta \gg 1$, the diffusion term can be ignored and conduction balanced against charge relaxation and convection. For steady motion, charge convection balances conduction when τ_C/τ_F is O(1).

Summary Equations for Leaky Dielectric Model

To summarize, the leaky dielectric electrohydrodynamic model consists of the following five equations. The derivation given here identifies the approximations in the leaky dielectric model. Except for the electrical body force terms,

it is essentially the model proposed by Melcher & Taylor (1969).

$$\frac{\tau_\mu}{\tau_P}\frac{\partial \mathbf{u}}{\partial t} + Re\mathbf{u}\cdot\nabla\mathbf{u} = -\nabla p - \frac{1}{2}\mathbf{E}\cdot\mathbf{E}\nabla\varepsilon + \nabla\cdot(\varepsilon\mathbf{E})\mathbf{E} + \nabla^2\mathbf{u} \quad \& \quad \nabla\cdot\mathbf{u} = 0 \tag{7′}$$

$$\nabla\cdot\sigma\mathbf{E} = 0 \tag{19′}$$

$$\frac{\tau_c}{\tau_P}\frac{\partial q}{\partial t} + \frac{\tau_c}{\tau_F}[\mathbf{u}\cdot\nabla_s q - q\mathbf{n}\cdot(\mathbf{n}\cdot\nabla)\mathbf{u}] = \| -\sigma\mathbf{E}\|\cdot\mathbf{n} \tag{22′}$$

$$\|\varepsilon\mathbf{E}\|\cdot\mathbf{n} = q \tag{3′}$$

$$\begin{aligned}[\boldsymbol{\sigma}^M\cdot\mathbf{n}]\cdot\mathbf{n} &= \frac{1}{2}\left\|\varepsilon(\mathbf{E}\cdot\mathbf{n})^2 - \varepsilon(\mathbf{E}\cdot\mathbf{t}_1)^2 - \varepsilon(\mathbf{E}\cdot\mathbf{t}_2)^2\right\| \\ [\boldsymbol{\sigma}^M\cdot\mathbf{n}]\cdot\mathbf{t_i} &= q\mathbf{E}\cdot\mathbf{t_i}\end{aligned} \tag{6}$$

Note that the equations are written in dimensionless variables using the scales defined in the text. The equation of motion is for nonhomogeneous fluids with electrical body forces. The hydrodynamic boundary conditions, continuity of velocity and stress, including the viscous and Maxwell stress, are assumed. Primes denote dimensionless forms of the parent equations.

Electrokinetic Effects

Although Equation 19 may be adequate for millimeter-length scales, it would fail if free charge on the Debye scale, $\kappa^{-1} \equiv \sqrt{\varepsilon\varepsilon_o k_B T/e^2\sum(z^k)^2 n^k}$, produces important mechanical effects. As noted earlier, charged interfaces attract counterions in the bulk fluid and repulse co-ions on the Debye length scale. Electric and hydrodynamic phenomena on this scale are responsible for the ubiquitous behavior of small particles in electrolytes, so it is natural to ask whether similar effects might be important here. In fact, Torza et al (1971) suggested that such effects could be responsible for the lack of agreement between the theory and their experiments on fluid globules.

To see whether the lack of agreement is due to electrokinetic effects we can use the numerical data already put forth. This leads to the following estimates: $\kappa^{-1} \approx 10^{-7}$ m, $\Lambda \approx 1$, $Pe\Lambda \approx 10^{-3}$, $Da \approx 10^{-4}$, $Da\sqrt{n^0/K} \approx 10^{-1}$ and $\beta = 10^{-1}$. Accordingly, on the Debye scale the relation between charge and field is represented by Equation 18 while the species conservation equations 12

become

$$\frac{\tau_D}{\tau_P}\frac{\partial n^1}{\partial t} = \omega^1 \nabla^2 n^1 \tag{23a}$$

$$\frac{\tau_D}{\tau_P}\frac{\partial n^k}{\partial t} = \beta \nabla \cdot [-z^k n^k \omega^k \mathbf{E}] + \omega^k \nabla^2 n^k + Da\sqrt{\frac{n^0}{K}}[n^1 - n^2 n^3], \quad k = 2, 3. \tag{23b}$$

These equations are clearly more complex than those for Ohmic conduction, which omits entirely any accounting for individual species. Is this complexity necessary? In the following sections, experimental and theoretical results based on the leaky dielectric model are reviewed for several prototypical problems so as to assess the model's effectiveness and the extent to which more detailed treatments taking account of diffuse layer effects are warranted. To date, none of the experimental studies show major electrokinetic effects despite the indications of the scale analysis.

FLUID GLOBULES

Drop Motion in External Fields

Allan & Mason (1962) encountered paradoxical behavior when non-conducting drops suspended in non-conducting liquids were deformed by a steady electric field. Conducting drops became prolate, as expected, but non-conducting drops often adopted oblate configurations. Oblate shapes were completely unexpected since analyses of static configurations predict prolate deformations, irrespective of the drop conductivity. Drop deformations can be analyzed with several methods. O'Konski & Thacher (1953) used an energy method; Allan & Mason (1962) balanced electrical and interfacial tension forces. For small deformations of conducting drops in dielectric surroundings, either procedure gives

$$D = \frac{9}{16}\frac{a\varepsilon\varepsilon_o E_\infty^2}{\gamma}. \tag{24}$$

Here E_∞ is the strength of the applied field, a is the drop radius, and γ is interfacial tension. The deformation, D, is the difference between the lengths of the drop parallel and transverse to the field divided by the sum of the two. Given that the drop is a conductor, it is easy to see why the shape is prolate since the pressures inside and outside the drop are uniform, initially, with the difference balanced by interfacial tension and the sphere's curvature, $2\gamma/a$. Therefore, non-uniform electric stresses must be balanced by interfacial tension on the

deformed surface. Since the sphere induces a dipole into the incident field, charge on the sphere's equipotential surface varies as $\cos\vartheta$; ϑ being measured from the direction of the field. The field normal to the surface varies in a similar fashion. Accordingly, the electric stress at the surface varies as $\cos^2\vartheta$, pulling the drop in opposite directions at its poles.

Dielectric drops in dielectric surroundings also become prolate in steady fields, irrespective of the dielectric constants of the two fluids, that is,

$$D = \frac{9}{16}\frac{a\varepsilon\varepsilon_o E_\infty^2}{\gamma}\frac{(\hat{\varepsilon}-\varepsilon)^2}{(\hat{\varepsilon}+2\varepsilon)^2} \tag{25}$$

with circumflexes denoting properties of the drop fluid (O'Konski & Thacher 1952, Allan & Mason 1962). Here deformation results from polarization forces since free charge is absent and the electric stresses are normal to the surface.

Allan & Mason's (1962) anomalous results led Taylor (1966) to discard the notion that the suspending fluids could be treated as insulators. Although the suspending fluids were poor conductors ($\sigma < 10^{-9}$ S/m) Taylor recognized that even a small conductivity would allow electric charge to reach the drop interface. With perfect dielectrics, the interface boundary condition (see Equation 3) sets the relation between the normal components of the field to ensure that there is no free charge. For leaky dielectrics, charge accumulates on the interface to adjust the field and ensure conservation of the current when the conductivities of the adjacent fluids differ. The action of the electric field on surface charge provides tangential stresses to be balanced by viscous flow. Taylor used the charge calculated from a solenoidal electric field to compute the electric forces at the interface of a drop and then balanced these stresses with those calculated for Stokes flow. This procedure led to a discriminating function to classify deformations as prolate or oblate:

$$\Phi = S(R^2+1) - 2 + 3(SR-1)\frac{2M+3}{5M+5}. \tag{26}$$

Here $S \equiv \varepsilon/\hat{\varepsilon}$, $R \equiv \hat{\sigma}/\sigma$, and $M \equiv \mu/\hat{\mu}$. Prolate deformations are indicated when $\Phi > 1$, and oblate forms are indicated when $\Phi < 1$. Qualitative agreement between theory and experiment was found in nine of the thirteen cases studied by Allan & Mason (1962). In the other four (prolate) cases, ambiguities in electrical properties hampered a test of the theory.

According to Taylor's leaky dielectric model, tangential electric stresses cause circulation patterns inside and outside the drop. As further confirmation of the theory, McEwan and de Jong[5] photographed tracer particle tracks in and around a silicone oil drop suspended in a mixture of castor and corn oils. Toroidal circulation patterns were observed, in agreement with the theory.

[5]McEwan & de Jong's photos are presented in an addendum to Taylor's paper (1966).

For a steady field, Taylor (1966) gives the deformation as

$$D = \frac{9}{16}\frac{a\varepsilon\varepsilon_o E_\infty^2}{\gamma}\Phi, \tag{27}$$

so it is possible to test the theory quantitatively by measuring the length and breadth of drops for small deformations. However, Taylor did not publish a comparison between theory and experiment. The first quantitative tests were reported by Torza et al (1971), who extended the leaky dielectric model to deal with oscillatory fields. The deformation ($0 < D < 0.1$) and burst of 22 fluid pairs were studied in steady and oscillatory (up to 60 Hz) fields. In steady fields, oblate deformations were observed in eight systems, in qualitative accord with the theory.

Although the qualitative aspects of the theory were vindicated, the quantitative agreement was very disappointing. The deformation always varied linearly with aE_∞^2, but the proportionality factor exceeded the theoretical value in all but one case, and the slopes were larger by a factor of two in more than half the systems. In one case, the measured slope was four times the theoretical value. In none of the systems was the measured slope less than the theoretical value, suggesting that the deviations are due to factors other than normal experimental errors.

Alternating fields offer additional insight into leaky dielectric behavior. As expected with alternating fields where forces vary as $aE_\infty^2\cos^2(\omega t)$, the deformation consists of steady and oscillatory parts (Torza et al 1971)

$$D = D_S + D_T. \tag{28}$$

The steady part, D_s, has the same form as Equation 27, but the Φ-function is

$$\Phi_S = 1 - \frac{S^2R(11+14M)+15S^2(1+M)+S(19+16M)+15R^2S\tau^2\omega^2(M+1)(S+2)}{5(M+1)[S^2(2+R)^2+R^2\tau^2\omega^2(1+S)^2]}, \tag{29}$$

where ω is the angular frequency, and τ represents a hybrid electrical relaxation time $\varepsilon_o\varepsilon/\hat{\sigma}$. According to Equation 29 the steady part of the deformation vanishes at a certain frequency and may shift from one form to the other with changes in frequency. Torza et al (1971) measured the steady part of the deformation for all 22 systems in 60-Hz fields and obtained results similar to those for steady fields. The deformation was proportional to aE_∞^2, and in five cases theory and experiment were in quantitative agreement. With the other systems the measured slopes exceeded the theoretical values by substantial margins. The transition from oblate to prolate deformation was reported for one system—a

silicone oil drop in sextolphthalate with $S \equiv \varepsilon/\hat{\varepsilon} \approx 2.2$ and $R \equiv \hat{\sigma}/\sigma < 0.07$. However, the observed transition frequency (1.6 Hz) was considerably lower than predicted (2.5 Hz), although the two could be brought into agreement by lowering S to 1.8. In this context the authors state: "This suggests that accurate measurements of the dielectric constants of the phases are crucial to a quantitative test of [the theory]." This observation will be revisited shortly.

Some of the disagreement about oscillatory fields could be ascribed to the omission of temporal acceleration. Torza et al (1971) used a quasi-steady approximation, tantamount to ignoring $\rho\partial\mathbf{u}/\partial t$ in the equations of motion. Upon including this acceleration, Sozou (1972) found qualitatively different behavior at high frequencies. For example, the steady part of the stress tends to zero, so this part of the deformation vanishes. With the quasi-steady approximation (see Equation 29), the deformation remains finite. Although this observation might account for some of the differences between theory and experiment in oscillatory fields, it does not resolve the low-frequency difficulties.

Torza et al's study (1971) provides additional confirmation of the qualitative aspects of the leaky dielectric model, but the lack of quantitative agreement is disconcerting. Even with water drops whose conductivity is five orders of magnitude larger than the suspending fluid, deviations between theory and experiment are substantial. Several reasons for the discrepancies were suggested. Lateral motion of charge along the interface due to surface conduction and convection of surface charge were ruled out since they ought to make the relation between deformation and aE_∞^2 nonlinear. Other possibilities were suggested: unspecified deviations from the boundary conditions, space charge in the bulk, and diffuse charge clouds due to counterion attraction (cf Equations 23a,b).

In an effort to address the boundary conditions issue, Ajayi (1978) employed perturbation methods to account for nonlinear effects in the deformation. This analysis represents the shape using a power series in $a\varepsilon\varepsilon_o E_\infty^2/\gamma$. By carrying the analysis through the second order in the small parameter, Ajayi found that $P_2(\cos\vartheta)$ and $P_4(\cos\vartheta)$ are required to represent the surface and the deformation is no longer directly proportional to $a\varepsilon\varepsilon_o E_\infty^2/\gamma$. Considering nonlinear effects helps to an extent, but Ajayi observed that "[the method] cannot remove the discrepancy between theory and experiment."

Another possibility advanced as a source of disagreement involves electrokinetic effects (Torza et al 1971). Given the results of the earlier scale analysis, this theory appeared worth investigating further. Baygents & Saville (1989) addressed the matter using asymptotic methods to account for the influence of a diffuse layer arising from coulomb interactions between current carrying ions and the surface charge. Three layers were identified where different processes dominate. A diffuse layer adjacent to the surface is separated from an outer region, where the leaky dielectric model applies, by an intermediate region. In

the diffuse layer, electrokinetic processes due to space charge are relevant. The intermediate region is electrically neutral, and charge transport by diffusion, electromigration, and convection are equally important. In the outer region, the electrohydrodynamic equations prevail. Solving the differential equations involved matched asymptotic expansions, and because of the altered structure of the problem, the distributions of velocity and stress differ from those derived using the leaky dielectric model. Nevertheless, the final expression for drop deformation is identical to that derived by Taylor (1966). Electrokinetic effects don't appear to contradict conclusions drawn from the leaky dielectric model, which, based on this analysis, appears to be an exact lumped parameter description.

Since none of the theoretical extensions appeared to resolve the divergence between theory and experiment, further experiments were undertaken. Following Torza et al's (1971) suggestion regarding the need for accurate dielectric constants and other properties (see above), Vizika & Saville (1992) paid careful attention to direct measurement of physical properties. They studied eleven different drop-host systems in steady fields; oscillatory fields were employed with five systems. The systems exhibited either prolate or oblate deformations. To increase the deformation, a non-ionic surfactant, Triton, was used in some cases to lower the interfacial tension. Generally speaking, agreement between theory and experiment improved over the earlier study. Figure 1 shows some results with steady fields. In all cases, D varied linearly with aE_∞^2.

Vizika & Saville (1992) observed time-dependent effects in some cases, especially with the surfactant. Evidently the fluids were not completely immiscible, and mass transfer occurred between phases. In these cases it was necessary to remeasure the properties after time had elapsed to permit equilibration. Moreover, in cases where the conductivities of the two phases were comparable, field-dependent effects were often observed.

In oscillatory fields, the steady part of the deformation was measured at different field strengths; D_S always varied linearly with aE_∞^2. The agreement between theory and experiment for the steady part of the deformation was generally better than with the same systems in a steady field. With water in castor oil, for example, the calculated and measured slopes differed by 34% in a steady field; in a 60-Hz field the two agreed. Figure 2 summarizes results with four systems.

Another interesting aspect of the leaky dielectric model concerns the effect of frequency. Torza et al (1971) showed, for example, that a drop that assumes an oblate deformation at low frequencies becomes prolate as the frequency increases, that is, $D_s/a\bar{E}_\infty^2$ increases with frequency. This behavior was measured with silicone drops suspended in castor oil; results are shown in Figure 3. The qualitative agreement between theory and experiment was

adequate, but as the figure indicates, the behavior is quite sensitive to the drop conductivity. Vizika & Saville (1992) compared theory and experiment for the oscillatory part of the deformation with one system; excellent agreement was obtained.

Further encouraging comparisons between theory and experiment were reported by Tsukada et al (1993), who studied deformations with the castor oil–silicone oil system. Castor oil drops in silicone oil gave prolate deformations, oblate deformations were found with the fluids reversed. In addition to experimental work, a finite element technique was employed to calculate deformations in steady fields. Except for the inclusion of finite deformations and

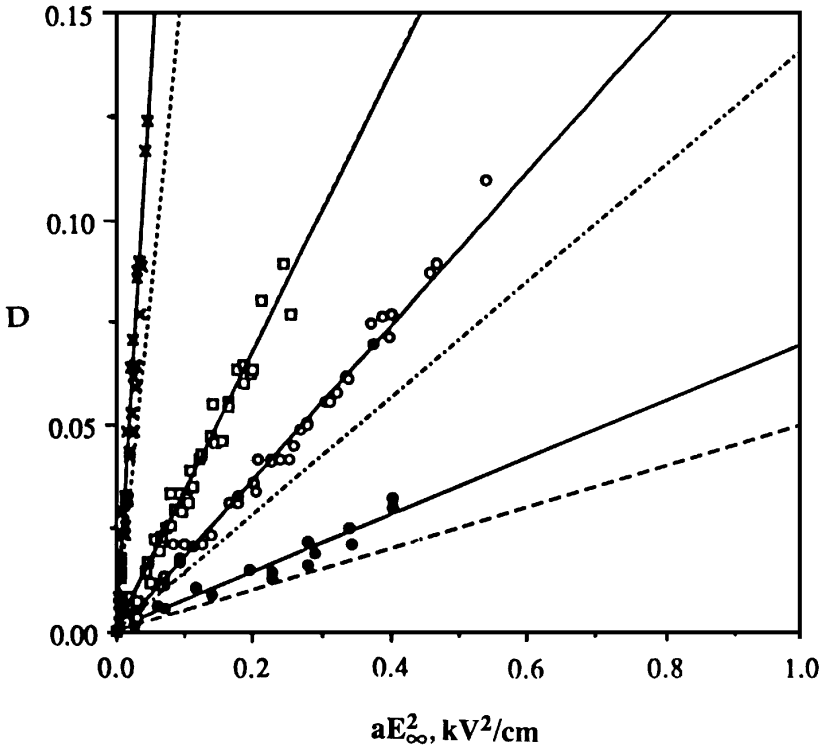

Figure 1 Deformation measurements for fluid drops (Vizika & Saville 1992). Drops are prolate or oblate depending on whether $D > 0$ or $D < 0$. The dashed lines represent calculations made with the leaky dielectric model using measured fluid properties; solid lines are least-squares representations of the experimental data. In Figure 1*b* the theoretical line for the upper set of data is not shown since it falls on the regression line for the lower data; for this system the difference between theory and experiment is large.

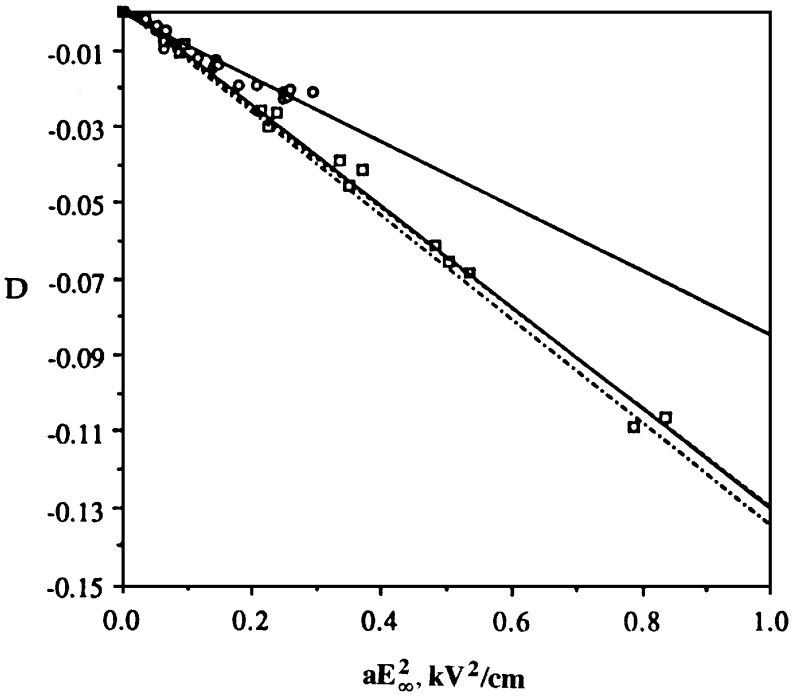

(b)

Figure 1 (*Continued*)

inertial effects, the standard leaky dielectric model was employed. At small deformations, numerical results agreed with those from Taylor's linear theory. With larger deformations, substantial differences appeared. Most of the differences between the finite element calculation and the linear theory were due to interface deformation since the Reynolds number in the calculations was always small. For prolate drops, the numerical results and Taylor's theory agreed with the experimental data for $0 < D < 0.07$. With larger deformations, for example, for $D \approx 0.2$, the finite element solution was better than the linear theory but still predicted smaller deformations than those observed. In addition, the agreement between Taylor's theory and the experiment for oblate drops exhibited a puzzling feature, that is, for large deformations the linear theory was closer to the experimental results than the nonlinear finite element calculation.

These three studies constitute the most comprehensive test of the theory wherein interface charge arises from conduction across an interface. The agreement between theory and experiment is encouraging, and there seems little doubt that, insofar as drop deformation is concerned, the theory does a satis-

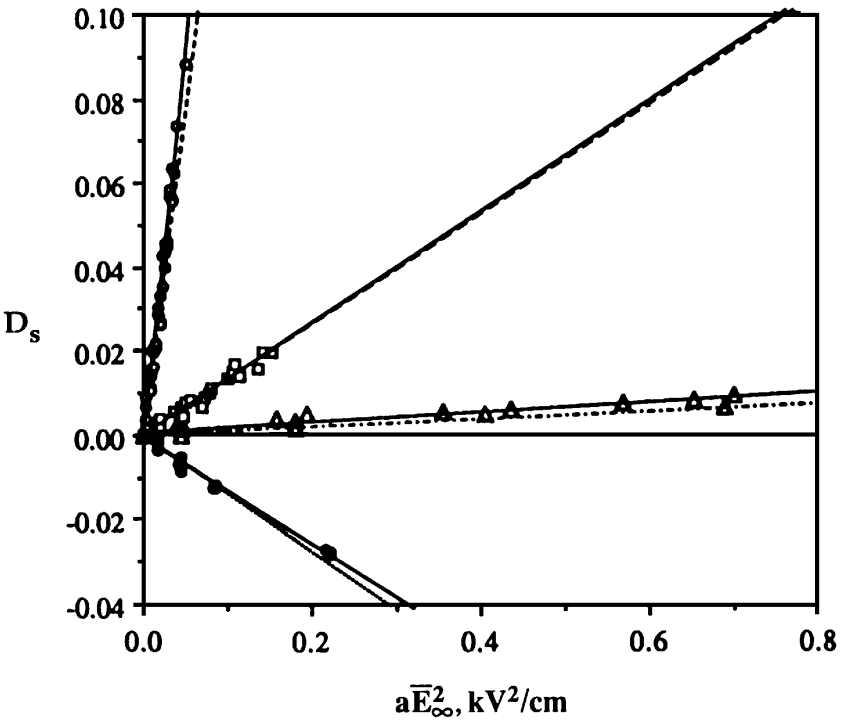

Figure 2 The steady part of the drop deformation in oscillatory fields (Vizika & Saville 1992).

factory job. Nevertheless, only a limited number of fluids have been studied, and even in these cases, conductivities have not been controlled. Questions as to finite amplitude effects or charge convection due to interface motion remain to be investigated.

In situations discussed thus far, charge convection has been ignored since $\tau_C/\tau_F \ll 1$. To investigate the influence of charge convection, the Hadamard-Rybczynski settling velocity for a spherical drop can be studied. Although no experimental studies exist, calculations with the model indicate a substantial influence. First note that the velocity will be unaltered if a steady field is imposed because, as long as charge convection is negligible, the net charge is zero and the field exerts no net force on the drop. However, an asymmetric charge distribution creates a net force; charge convection due to sedimentation generates the necessary asymmetry. The relevant boundary condition is Equation 22′ rewritten for steady flow,

$$\frac{\tau_c}{\tau_F}\nabla_s \cdot (\mathbf{u}q) = \|-\sigma\mathbf{E}\| \cdot \mathbf{n}. \tag{30}$$

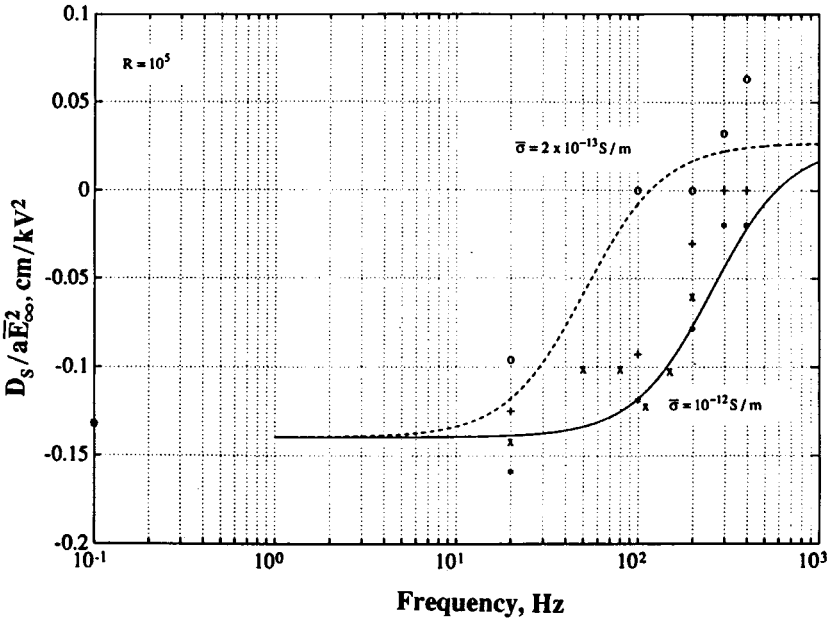

Figure 3 The unsteady part of the drop deformation as a function of frequency for silicone drops in castor oil (Vizika & Saville 1992). Torza et al's (1971) theoretical result is shown for two values of the drop conductivity; other parameters correspond with measured values.

Here the flow time will be $a/u_o = \mu/\varepsilon\varepsilon_o E_\infty^2$, so $\tau_C/\tau_F = (\varepsilon\varepsilon_o E_\infty)^2/\mu\sigma \cdot \tau_C/\tau_F \approx 0.1$ for $\varepsilon = 4$, $\mu = 10^{-1}$ N-m, $\sigma = 10^{-9}$ S/m, and $E_\infty = 10^5$ V/m, so a linearized treatment is appropriate (Spertell & Saville 1976). Solving the equations shows the settling velocity is retarded or increased depending on the electrical relaxation times in the two fluids, that is,

$$U = \frac{3U_{\text{st}}}{\frac{3+2M}{1+M} + \frac{(\varepsilon\varepsilon_o E_\infty)^2}{\sigma\mu} F(R, S, M)}. \tag{31}$$

U_{st} is the Stokes settling velocity for a rigid sphere and

$$F(R, S, M) = \frac{6M^2[3S(R+1) - 1][RS - 1]}{5(1+M)^2 S^2 (3+2R)(2+R)^2}. \tag{32}$$

Also, with charge convection, drop deformation is no longer symmetric with respect to the midplane. These results show clearly that charge convection has different effects, either enhancing or retarding sedimentation, depending on the charge relaxation times in the two fluids.

Given that interface charge induced by the action of an electric field in leaky dielectrics has important effects on quasi-static motions, the next task is to inquire as to its effects on drop stability.

Drop Stability and Breakup

To provide a context to study the role of tangential stresses it is helpful to recall work on perfect conductors and dielectrics. Studies of drop dynamics[6] and stability began with Rayleigh's celebrated 1882 paper "On the equilibrium of liquid conducting masses charged with electricity." His analysis pertains to instantaneous charge relaxation inside an isolated drop, and the relation[7] between the frequency, ω, interfacial tension, γ, and drop charge, Q, is

$$\omega^2 = n(n-1)\left\{(n+2)\frac{\gamma}{\rho a^3} - \frac{Q^2}{16\pi^2\varepsilon_o\rho a^6}\right\} \tag{33}$$

for axisymmetric oscillations of an inviscid drop of radius a and density ρ. Here n denotes the index of the Legendre polynomial $P_n(\cos\vartheta)$. For perfectly conducting fluids, the electric stress is wholly normal to the interface. Instability occurs for $n = 2$ when the charge increases to a level where the expression in brackets vanishes. Because a linearized, spheroidal approximation is used, either oblate or prolate deformations are included. Although the Rayleigh limit pertains strictly to small oscillations, dimensional analysis shows that the criterion for instability will still be of the form

$$\frac{Q^2}{\varepsilon_o a^3\gamma} > C, \tag{34}$$

but the constant C will depend on the properties of the surrounding fluid.

An EHD model of a leaky dielectric drop oscillating in an insulating fluid addresses effects of charge relaxation inside the drop through a boundary condition for the conservation of interfacial charge, q. Accordingly, the model consists of linearized[8] equations of motion for incompressible fluids inside and outside the drop,

$$\frac{\tau_\mu}{\tau_p}\frac{\partial\mathbf{u}}{\partial t} = -\nabla p + \nabla^2\mathbf{u}, \quad \nabla\cdot\mathbf{u} = 0, \tag{35}$$

relations between the field and the current in each phase,

$$\nabla\cdot\mathbf{E} = \mathbf{0}, \quad \nabla\times\mathbf{E} = \mathbf{0}, \tag{36}$$

[6]Rayleigh's *Theory of Sound* (1945) contains many fascinating accounts of early work on drops and cylinders.

[7]Recall that the rationalized MKSC system is used here. In Rayleigh's notation, $\varepsilon_o = 1/4\pi$.

[8]The linearization is based on the size of the deformation relative to the undeformed drop.

and boundary conditions. The relation between field and charge is given by the dimensionless form of Equation 3,

$$\|\varepsilon \mathbf{E}\| \cdot \mathbf{n} = q, \tag{37}$$

with charge scaled on the charge density on the undeformed drop, $Q/4\pi a^2$. The scale for the electric field, E_o, is $Q/4\pi\varepsilon_o a^2$. Charge on the interface is conserved, and for $\beta \gg 1$ the balance is

$$\frac{\tau_c}{\tau_P}\frac{\partial q}{\partial t} + \frac{\tau_c}{\tau_F}[\mathbf{u}\cdot\nabla_s q - q\mathbf{n}\cdot(\mathbf{n}\cdot\nabla)\mathbf{u}] = (\omega^2 n^2 + \omega^3 n^3)\mathbf{E}\cdot\mathbf{n}. \tag{38}$$

To conserve charge, ion mobilities in the outer fluid must be zero so that the current on the right-hand side represents conduction from the interior. For Rayleigh's perfectly conducting drop, the local charge balance is unnecessary because: (*a*) the field is nil inside the drop, and (*b*) charge transport is instantaneous so that the convection and relaxation terms vanish. The remaining boundary conditions are continuity of velocity and stress, and the kinematic condition.

These equations have been solved to investigate how relaxation alters Rayleigh's results (Saville 1974). Both viscous forces and charge relaxation effects were included, but general conclusions were obscured by the awkward transcendental form of the characteristic equation. However, asymptotic methods can be used to identify the salient features. The result for a slightly viscous drop in the absence of a suspending fluid is rather surprising in as much as Rayleigh's result (see Equation 33) is recovered as the stability criterion. Even when charge relaxation by conduction is slow, charge convection still redistributes charge so rapidly that the oscillation frequency is given by Equation 33. A similar explanation was proposed by Melcher & Schwartz (1968) in their study of planar interfaces. Although EHD effects fail to alter the oscillation frequency, damping rates are affected. If the damping rate is denoted as δ, then the amplitude of the oscillation decays as $\exp[(i\omega_R - \delta)t]$; ω_R represents the Rayleigh frequencies from Equation 33.

First, note that with instantaneous relaxation the damping is volumetric and Rayleigh's theory gives

$$\delta \approx (2n+1)(n-1)\frac{\nu}{a^2} \quad \text{for} \quad \left[\frac{a\gamma}{\rho\nu^2}\right]^{\frac{1}{2}} \gg 1 \tag{39}$$

for a drop with kinematic viscosity ν. When electrohydrodynamic effects are included and the oscillation time is comparable to the conduction time, that is when $\varepsilon\varepsilon_o\omega_o/\sigma \approx \mathrm{O}(1)$, damping is slower:

$$\delta \approx (2n-3)(n-1)\frac{\nu}{a^2}. \tag{40}$$

Other interesting effects can be identified, including modes involving rapid damping in a thin boundary layer where the rate is proportional to $(a\gamma/\rho\nu^2)^{\frac{2}{3}}$.

Rayleigh's criterion also applies to very viscous drops with rapid charge relaxation. In contrast, slow charge relaxation, that is, $\varepsilon\varepsilon_o/\sigma \gg a\rho\nu/\gamma$, has a substantial effect on highly viscous systems. Here the criterion for stability is altered to

$$\frac{Q^2}{16\pi^2 a^3 \varepsilon_o \varepsilon \gamma} > \frac{40\hat{\varepsilon} + 180\varepsilon}{10\hat{\varepsilon} + 9\varepsilon} \tag{41}$$

for a viscous drop with dielectric constant $\hat{\varepsilon}$ and viscosity $\hat{\mu}$ in a fluid with ε and μ where $\hat{\mu} \gg \mu$ and $(a\gamma/\hat{\rho}\hat{\nu}^2)^{\frac{1}{2}} \ll 1$. The next topic concerns behavior beyond the range where a linear treatment is acceptable.

To form a simple model, the breakup of isolated drops or drops in external fields can be treated by approximate methods. A spheroidal approximation (Taylor 1964) yields an accurate expression for the stability of an isolated charged drop or an uncharged drop in an external field. More recent work[9] shows that prolate shapes evolving below the Rayleigh limit are unstable to axisymmetric perturbations while oblate shapes above the limit are stable to axisymmetric perturbations but unstable to nonaxisymmetric perturbations. Thus, the Rayleigh limit turns out to be the absolute limit of stability.

Dimensional analysis indicates that the criterion for instability of a conducting drop immersed in a gas and stressed by an external field has the form

$$\frac{a\varepsilon_o E_\infty^2}{\gamma} > C. \tag{42}$$

Taylor's spheroidal approximation (Taylor 1964) gives $C = 2.1 \times 10^{-3}$ for $D = 0.31$, in good agreement with experiments on soap films. The limiting deformation corresponds to a drop with an aspect ratio of 1.9. Above this point the drop is seen to throw off liquid as a fine jet.

Taylor (1964) analyzed the region near the spheroidal tip, which becomes conical (a "Taylor cone") at the limit of stability. For a cone with a vertex angle of 98.6°, electric stresses on a conducting surface are balanced exactly by surface tension. It turns out that conical tips also exist as static solutions when one perfect dielectric is immersed in another and $S \equiv \varepsilon/\hat{\varepsilon} \leq 17.6$ (Ramos & Castellanos 1994a). At the limit the vertex angle is 60°. For $S < 17.6$, two solutions exist. One has a vertex angle larger than 60°; the other is smaller. At $S = 0$ the vertex angles are 0 and 98.6°, the latter corresponding to Taylor's solution for an equipotential cone.

[9]Pelekasis et al (1990) and Kang (1993) provide useful summaries of the dynamical stability of perfectly conducting drops.

More extensive analyses of the static behavior of drops disclose behavior consistent with this picture: Sherwood (1988, 1991) studied free drops; Wohlhuter & Basaran (1992) and Ramos & Castellanos (1994b) analyzed drops pinned to an electrode. According to the various computations, a dielectric drop immersed in another perfect dielectric elongates into an equilibrium shape as the field increases when $S > S_1$. For $S > S_2 > S_1$ the drops become unstable at turning points in the deformation-field strength relation. In the range $S_1 > S > S_2$ there is hysteresis; drops are stable on the lower and upper branches of the relation and unstable in between. Values of S_2 calculated by various methods are close to the value identified as the maximum value for the existence of a cone. Wohlhuter & Basaran (1992) and Ramos & Castellanos (1994b), who studied pendant and sessile drops between plates, delineate other quantitative effects due to contact angle, drop volume, and plate spacing.

How do EHD phenomena modify this picture? Interestingly, solutions for a leaky dielectric cone immersed in another leaky dielectric fluid exist for $R \equiv \hat{\sigma}/\sigma > 17.6$, independent of the dielectric constants (Ramos & Castellanos 1994a). Because of tangential stresses, the fluids are in motion (Hayati 1992). As before the cone angle is less than 60°, and two solutions exist as long as the conductivity ratio is large enough. The balance between electrical stress and interfacial tension determines the cone angle, and the normal component of the viscous stress is zero. As required, the tangential electric stress along the periphery of the cone is balanced by viscous stress. A circulation pattern exists inside and outside the cone with fluid moving toward the apex along the interface and away from it along the axis. One might conjecture that a certain level of conductivity is necessary for the formation of a sharp point and the ensuing micro-jet (see below).

Allan & Mason (1962) and Torza et al (1971) observed three modes of drop deformation and breakup at high field-strengths: (*a*) water drops in oil deformed symmetrically, and globules pinched off from a liquid thread; (*b*) castor oil drops in silicone oil deformed asymmetrically with a long thread pulled out toward the negative electrode; and (*c*) silicone oil drops in castor oil flattened and broken up unevenly. For modes *a* and *b* the initial deformation was prolate; for mode *c* it was oblate. The breakup of oblate drops in steady fields involved a complex folding motion with a doughnut-like shape. In an oscillatory field, small drops were ejected from part of the periphery.

Sherwood (1988) dealt with symmetric deformations (mode *a*) using a boundary integral technique. Perfect conductors or perfect dielectrics deform into prolate shapes in steady fields. With perfect conductors, the tips have a small radius of curvature, and Sherwood's algorithm predicts breakup at the tip with critical field-strengths close to those found by Taylor (1964) and Brazier-Smith (1971). Perfect dielectrics display similar overall behavior, and the maximum

aspect ratio is near that predicted by energy arguments. With the leaky dielectric model, drops elongate and take on a shape with fattened ends connected by a thin neck. Since the calculation is quasi-static, transient behavior can be followed in cases where breakup occurs. Here the leaky dielectric model depicts drop elongation followed by breakup into individual droplets, behavior consistent with experimental results. In a leaky dielectric, electrohydrodynamic stresses flatten the almost-conical tips formed in perfect dielectrics or conductors. Sherwood defines two sorts of drop breakup: the electrostatic mode where a conical tip develops and breakup is via *tip-streaming*, and the EHD mode following instability of the elongated thread. Because of the numerical algorithm's structure it was not possible to study the other mode of breakup identified by Torza et al (1971), which remains a subject for future study along with effects of viscosity. Curiously, conical tips of the sort identified by Ramos & Castellanos (1994a) were not found in Sherwood's calculation.

Following tip geometry much beyond the point of instability has not been possible although Basaran et al (1995) report detecting embryonic jets. Their computation includes dynamic effects with fluid inertia balanced against interfacial tension and electrostatic forces. Although the focus is on perfect conductors and inviscid fluids, small jets were identified emanating from the tips. Inasmuch as electrohydrodynamic effects appeared to suppress conical tip formation (Sherwood 1988), much more effort will be required to resolve the issue of jet creation. In calculations to date, perfectly conducting, inviscid drops produce (immature) jets; viscous, leaky dielectric drops do not.

Predicting the onset and structure of the thin jet emerging from a Taylor cone is difficult, but EHD processes are clearly involved. Observations of liquid drops emerging from a small capillary make this conclusion abundantly clear. Drops become smaller as the potential is raised, and when the potential reaches a certain level, the drops emerge in a pulsating fashion. With further increases in the potential, the drop develops a Taylor cone that has a jet emerging from its tip. According to Hayati et al (1986, 1987a,b) and Cloupeau & Prunet-Foch (1990), effective atomization is possible only when the liquid conductivity lies in a certain range. To first order, the flow pattern inside the cone can be approximated by superimposing flow into a conical sink onto the conical flow driven by a tangential electric stress varying as r^{-2}. The tangential stress arises from charge conduction to the interface. Charge accumulation stems from differences between the conductivity of the interior and exterior fluids. The flow pattern has a somewhat counterintuitive structure: Liquid is supplied to the jet from the surface of the cone, while a recirculating eddy moves fluid down the axis of the cone toward the supply. Of course this analysis omits details of the jet, whose characteristics are submerged in the singularity at the cone tip. Accounting for charge convection on the surface of the cone, which clearly

becomes important near the apex (Ramos & Castellanos 1994b, Fernandez de la Mora & Loscertales 1994), has eluded analysis to date.

FLUID CYLINDERS

Stability of Charged Cylinders (Free Jets)

Shortly after Rayleigh's pioneering paper (Rayleigh 1882), Bassett (1894) showed how charge destabilizes a cylinder by a mechanism similar to that found earlier with drops. Nevertheless, the process is more complex because a cylinder may be unstable even in the absence of electrical forces. If the wavelength of a corrugation exceeds the circumference, then a varicose surface may have a smaller area than a circular cylinder and be unstable because it has a lower (free) energy. By studying the dynamics of a charged, inviscid cylinder, Bassett showed that an axisymmetric disturbance of wavelength λ will grow if

$$\frac{\alpha I_o'(\alpha)}{I_o(\alpha)}\left[1-\alpha^2-\frac{a\varepsilon_o E_\infty^2}{\gamma}\left[1+\alpha\frac{K_o'(\alpha)}{K_o(\alpha)}\right]\right]>0. \tag{43}$$

Here $\alpha \equiv 2\pi a/\lambda$, a is the radius, $I_m()$ and $K_m()$ denote modified Bessel functions of order m with the prime sign denoting differentiation, and E_∞ is the (radial) field strength at the surface. When the inequality fails, the cylinder oscillates. The quantity on the left of Equation 42 is proportional to the growth rate when the cylinder is unstable and to the oscillation frequency when it is stable. For an uncharged cylinder, instability is indicated when $\alpha < 1$, that is, when $\lambda > 2\pi a$. Electric charge expands the range of unstable wave numbers and increases growth rates. For $a\varepsilon_o E_\infty^2/\gamma = 1$, the range is approximately $0 < \alpha < 1.35$ ($\lambda > 1.5\pi a$). Interestingly, charge destabilizes non-axisymmetric deformations that are otherwise stable; the relation for these modes may be obtained from Equation 42 by equating the index of the Bessel functions with the mode for the angular deformation, $\cos(m\vartheta)$, and changing $1-\alpha^2$ to $1-\alpha^2-m^2$. Viscous effects dampen the motion, but their effect is such as to make some non-axisymmetric motions relatively more unstable (Saville 1971a). The theory for charged cylinders is in qualitative accord with Huebner's (1969) finding of non-axisymmetric modes of breakup with highly charged water jets. Similar behavior exists with highly viscous cylinders, where, in addition to destabilizing non-axisymmetric modes, the presence of charge lowers the wavelength of the most unstable mode. Charge relaxation on an initially uniformly charged jet does not appear to have been studied, although given the importance this process has with axial fields, the topic is of considerable interest.

Taylor (1964) observed that "induced charge has a very powerful effect in preventing the break up of jets into drops under certain circumstances and an equally powerful effect in causing violently unsteady movements ultimately

disintegrating the jet into drops in others." Taylor was referring to the effects of a field aligned with the axis of a water jet. Raco's (1968) experiments with poorly conducting liquids also show a strong stabilizing effect. These results produce a quandary of sorts. Axial fields promote stability with dielectric jets (Nayyar & Murthy 1960) because of the action of the normal component of the electric field on the deformed interface. But the required field strengths are much larger than those encountered by Taylor, and the dual nature of electric forces noted by Taylor does not appear to be consistent with the behavior of perfect dielectrics.

The role of electric stress can be appreciated by imagining an axisymmetric deformation of the surface of the form $1 + \zeta(z, t)$. The normal component of the electric stress on the interface of a perfect dielectric due to axial field is

$$-\frac{a\varepsilon\varepsilon_o E_\infty^2}{\gamma}\frac{(1-\hat{\varepsilon}/\varepsilon)^2}{I_o(\alpha)K_1(\alpha)+\hat{\varepsilon}/\varepsilon I_o(\alpha)K_1(\alpha)}\alpha\zeta(z,t), \tag{44}$$

where the dielectric constants of the cylinder and outer fluid are denoted by $\hat{\varepsilon}$ and ε. Thus protrusions are pushed inward and depressions outward irrespective of the wavelength of the disturbance. In contrast, the normal stress on a charged, conducting cylinder is

$$-\frac{a\varepsilon\varepsilon_o E_\infty^2}{\gamma}\left[1-\frac{\alpha K_1(\alpha)}{K_o(\alpha)}\right]\alpha\zeta(z,t), \tag{45}$$

so this stress resists deformation only when the term in brackets is positive, that is, for $\alpha < 0.6$. Moreover, with perfectly conducting fluids some wavelengths are made more unstable. Although axial fields are seen to promote stability with dielectrics, large wavelengths (small α's) remain unstable. Since the stresses with perfect conductors or dielectrics are normal to the interface, the situation should be different with leaky dielectric materials due to tangential EHD stresses.

The leaky dielectric equations have been solved for a viscous cylinder immersed in another viscous liquid under conditions where the current is continuous at the interface, that is, ignoring charge transport by relaxation, convection, and dilation of the surface. In terms of the dimensionless parameters in Equation 22′, $\tau_C \ll \tau_P \,\&\, \tau_F$. If, for example, we choose the process time to be the hydrodynamic time and identify it as that for a relatively inviscid material, $(\hat{\rho}a^3/\gamma)^{1/2}$, then $\hat{\varepsilon}\varepsilon_o/\hat{\sigma}\,(\hat{\rho}a^3/\gamma)^{1/2} \ll 1$. For distilled water, the electrical relaxation time is less than a millisecond and the hydrodynamic time for a 1-mm water jet is over a second; for apolar liquids of the sort mentioned earlier, the relaxation time may be longer ($\approx$35 ms). In either case $\tau_C \ll \tau_P$, so the approximation is appropriate. With leaky dielectrics the normal stress differs from that noted with perfect dielectrics, and there is also a tangential

stress due to induced charge. Before deformation the surface is free of charge since the field is parallel to the surface. Upon deformation, the interface tilts in the field and conduction processes induce charge. The normal stress is proportional to

$$-\frac{a\varepsilon\varepsilon_o E_\infty^2}{\gamma}\frac{(1-\hat{\sigma}/\sigma)(1-\hat{\varepsilon}/\varepsilon)}{I_o(\alpha)K_1(\alpha)+\hat{\sigma}/\sigma\, I_o(\alpha)K_1(\alpha)} I_o(\alpha)K_o(\alpha)\alpha\zeta(z,t), \tag{46}$$

and the tangential stress induced by the deformation is proportional to

$$-\frac{a\varepsilon\varepsilon_o E_\infty^2}{\gamma}\frac{(\hat{\sigma}/\sigma-\hat{\varepsilon}/\varepsilon)}{I_o(\alpha)K_1(\alpha)+\hat{\varepsilon}/\varepsilon I_o(\alpha)K_1(\alpha)}\zeta(z,t). \tag{47}$$

So the sense of the stress depends on the relative magnitudes of both the electrical conductivities and the dielectric constants. However, the combined action of the two stresses makes it possible to stabilize the cylinder to disturbances of any wave number with smaller fields than those needed with perfect dielectrics (Saville 1970; Mestel 1994, 1996).

Figure 4 shows the growth rate parameter, ω, for a disturbance growing as $\exp(\omega t)$. Note that a value of $a\varepsilon\varepsilon_o E_\infty^2/\gamma$ slightly larger than 0.005 suffices to stabilize the cylinder for $\hat{\varepsilon}/\varepsilon = 78$. This result is encouraging since Taylor found a water jet was stable with $a\varepsilon\varepsilon_o E_\infty^2/\gamma \approx 0.005$ and unstable when $a\varepsilon\varepsilon_o E_\infty^2/\gamma$ was lowered to 0.003. Cylinders with smaller dielectric constants require larger fields, as would be expected from the amount of charge conducted to the interface by a deformation. For $\hat{\varepsilon}/\varepsilon = 2$, stability requires $a\varepsilon\varepsilon_o E_\infty^2/\gamma > 0.03$.

Axially directed fields completely stabilize highly viscous cylinders (Saville 1970, Mestel 1995). Recall that when viscous effects dominate, infinitely long wavelengths are the most unstable when capillary forces operate alone on the interface. Whatever the viscosity, EHD effects produce both tangential and normal stresses so that with highly viscous cylinders the main issues are quantitative. Analysis shows that stability of a highly viscous cylinder is ensured when

$$\frac{a\varepsilon\varepsilon_o E_\infty^2}{\gamma}(\hat{\sigma}/\sigma-\hat{\varepsilon}/\varepsilon) \geq \frac{1}{2}. \tag{48}$$

Intermediate situations where the mechanical properties of both cylinder and surroundings are included are best investigated numerically using the characteristic equation in its implicit form (Saville 1970).

Although the leaky dielectric model with rapid relaxation of surface charge shows promise in conjunction with the behavior encountered in Taylor's (1969) experiments, it still fails to capture the oscillatory behavior noted upon increasing the field. One means of addressing this matter is to include charge relaxation

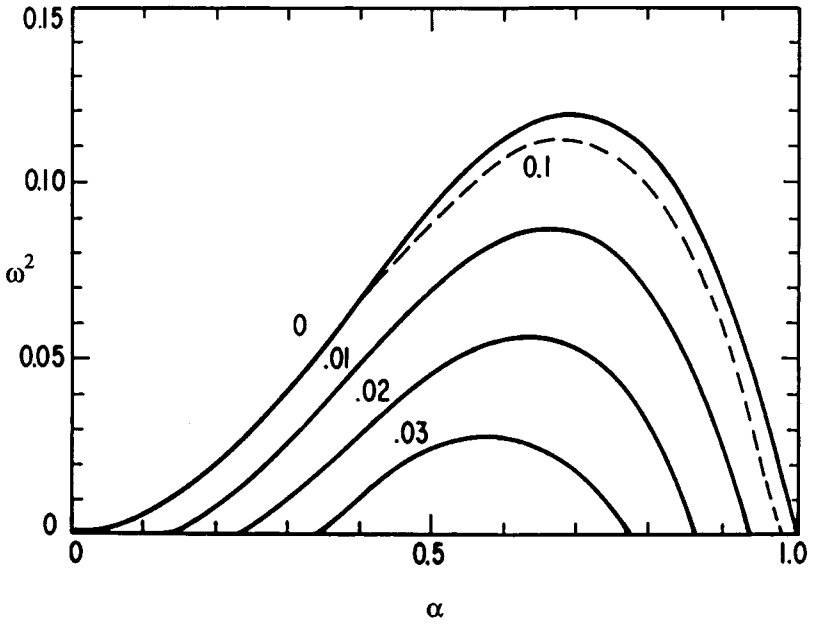

Figure 4 The stability parameter, ω^2, for a slightly viscous leaky dielectric cylinder in an axial field as a function of the wave number of the deformation, α, for $\hat{\varepsilon}/\varepsilon = 2$ (Saville 1971b) and various values of $a\hat{\varepsilon}\varepsilon_o E_\infty^2/\gamma$. The dashed line represents behavior of a perfect dielectric with $a\hat{\varepsilon}\varepsilon_o E_\infty^2/\gamma = 0.1$.

by using Equation 22′ in the form

$$\frac{\tau_c}{\tau_P}\frac{\partial q}{\partial t} = \|-\sigma\mathbf{E}\| \cdot \mathbf{n}, \qquad (22'')$$

with $\tau_R \equiv \tau_c/\tau_P \equiv (\hat{\varepsilon}\varepsilon_o/\hat{\sigma})/(\hat{\rho}a^3/\gamma)^{1/2}$. For the stability problem, charge convection and dilation of the interface remain negligible because the problem is linearized for small disturbances; that is, both the velocity and the interface charge are proportional to the size of the deformation. Solutions of the model equations for a viscous jet with Equation 22″ as the boundary condition for charge show several interesting features (Saville 1971b). For relatively good conductors (instantaneous relaxation: $\tau_R \approx 0$), the earlier results for leaky dielectrics are recovered and non-axisymmetric deformations are always stable. With less conductive material (slow relaxation: $\tau_R \gg 1$), perfect dielectric behavior results and wave numbers in the range 0–α^*, where $\alpha^* < 1$, are unstable no matter how high the field. When τ_R is 0(1), new sorts of behavior are found.

As expected, EHD effects tend to stabilize the axisymmetric mode, but not completely and only up to a certain value of $a\varepsilon\varepsilon_o E_\infty^2/\gamma$. With $\tau_R = 0.5$, the growth rate of the most unstable axisymmetric mode diminishes by a factor of 28 for $a\varepsilon\varepsilon_o E_\infty^2/\gamma = 0.005$, whereas a field of this size would completely stabilize the jet if charge relaxed instantaneously. In addition, the wavelength is diminished by more than a factor of 2 and growth is oscillatory. Further increases in $a\varepsilon\varepsilon_o E_\infty^2/\gamma$ increase growth rates and oscillation frequencies slowly. Equally important, however, non-axisymmetric modes are destabilized; similar behavior was found earlier with perfectly conducting jets. Thus, the *whipping mode* ($m = 1$) becomes unstable as do modes associated with alteration of the cross section ($m = 2, \ldots$). Taylor (1969) found that increasing the field strength first tended to stabilize and then destabilize jets in axial fields. Moreover, the instability was manifested by a sideways motion of the liquid filament. These observations are for moderately viscous materials. With highly viscous jets, charge relaxation causes the varicose instability to become oscillatory.

The next step in the analysis of jet stability involves surface charge in the base state to encompass, for example, the behavior of a cone-jet emanating from a droplet. As noted earlier, droplets adopt conical tips from which a thin jet emanates and transports surface charge induced upstream of the cone. Mestel (1994, 1996) has analyzed the behavior of slightly viscous and highly viscous fluid jets with surface charge. These situations differ from the earlier work in two important aspects. First, due to the presence of charge in the base state, transport by convection and dilation of the surface must be included in the boundary condition along with relaxation and conduction to the surface. Second, the presence of surface charge mandates shear in the unperturbed flow. The analysis requires deft use of asymptotic methods. Mestel (1994) has shown that shear tends to stabilize the jet, as long as it is not too strong. Charge in the base state, per se, enhances instability, as might be expected, but charge with a small tangential field is stabilizing.

Interesting behavior is also encountered for highly viscous jets where the base state shear field fills the cross section. For a fixed amount of surface charge in the base state, the jet is unstable, but adding an axial field stabilizes the system depending on the size of the relaxation time-scale parameter, $\tau_R \equiv \hat{\varepsilon}\varepsilon_o\gamma/\hat{\sigma}a\mu$. With $\tau_R \neq 0$, it is possible to completely stabilize the jet against axisymmetric instabilities with a sufficiently high field only if the surface charge is in an appropriate range (Mestel 1996).

Studies of free jets (Taylor 1969) disclosed fascinating behavior in the presence of an axial field, and the qualitative predictions of the leaky dielectric model are consistent with the limited experimental data. As a first approximation the leaky dielectric model furnishes a picture superior to that formed

treating the fluid as a perfect dielectric. However, interfacial charge relaxation and convection processes need to be taken into account to provide a comprehensive description. Recent studies suggest a rich variety of phenomena that warrant study.

Stability of Pinned Cylinders (Liquid Bridges)

Fluid cylinders with pinned contact lines furnish another configuration for study, especially when the cylinder is surrounded by a matched density fluid to circumvent buoyancy. Because of their importance as venues for crystal growth, considerable effort has been devoted to the study of liquid bridges (Hurle et al 1987). For our purposes they offer an ideal configuration to compare theory and experiment. As Plateau noted, a liquid column is stable insofar as its circumference exceeds its length. Put another way, the column is stable as long as its aspect ratio (L/d) is less than π. Here, electric forces play roles similar to those encountered with jets, but study along these lines is only just beginning.

Gonzalez et al (1989) studied the behavior of an almost isopycnic system and provided the first theoretical treatment of perfect dielectric behavior. In their experiment, a 50-Hz field aligned with the axis of the bridge was used to stabilize columns with aspect ratios larger than π. The alternating field tends to suppress effects due to interface charge and thus achieves perfect dielectric behavior. Here the stability boundaries depend on three dimensionless parameters: the aspect ratio (L/d), the dielectric constant ratio ($\hat{\varepsilon}/\varepsilon$), and the ratio of electric stress to surface tension ($a\varepsilon\varepsilon_o E_\infty^2/\gamma$). There are even and odd modes of deformation, and the form that is asymmetric to the mid-plane is least stable. Because of the way the dielectric constant ratio enters the stability criterion (cf Equation 44), the arrangement of fluids has almost no effect on the instability boundary. This is in sharp contrast with the situation for leaky dielectrics where interchanging fluids has a marked effect as seen from Equations 46 and 47. Figure 5 depicts a comparison between the linearized theory and experiment for a castor oil–silicone oil system. The poor agreement for $L/d \approx \pi$ appears to be due to the density mismatch (Gonzalez & Castellanos 1993, Ramos et al 1994).

Leaky dielectric behavior was studied using steady fields with castor oil–silicone oil systems by Sankaran & Saville (1993), who identified two transitions: departure from a perfect cylinder and pinch-off. These transitions are separated by a wide margin as shown in Figure 6. As Figures 5 and 6 show, leaky dielectrics require lower field strengths than do perfect dielectrics. Equations 46 and 47 reveal that, providing the ratios of conductivities and dielectric constants have the proper magnitudes, interchanging the bridge and bath fluids can reverse the signs of the normal and tangential stresses. Hence, a

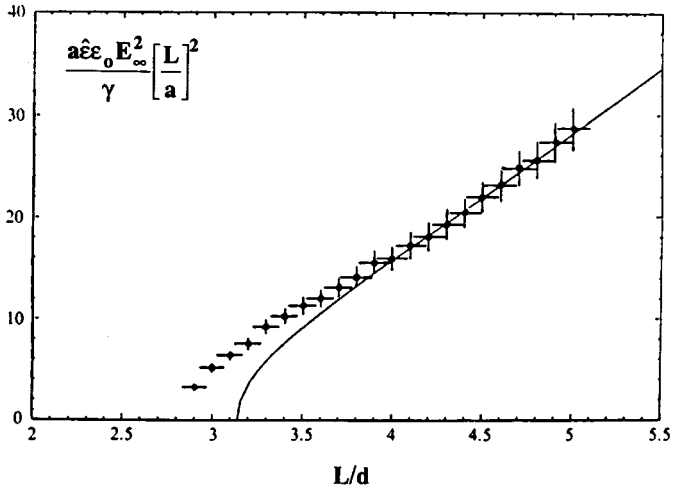

Figure 5 The behavior of a liquid bridge in 50-Hz axial fields (Gonzalez et al 1989). The line shows the boundary between stability and instability calculated for a perfect dielectric. According to theory and experiment the arrangement of the fluids is immaterial; either may be used as the bridge with little change in the boundary.

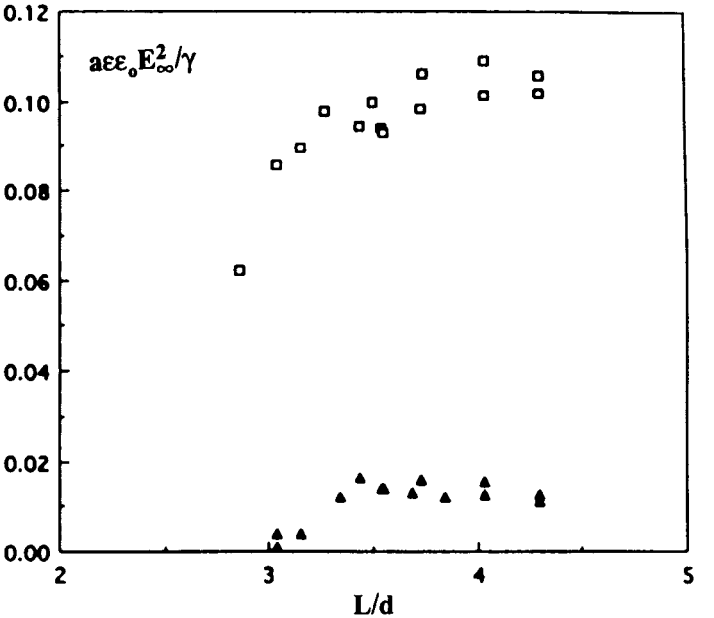

Figure 6 Stability boundaries for leaky dielectric bridges (castor oil in silicone oil) in steady fields as functions of the aspect ratio (Sankaran & Saville 1993). Upper points denote the perfect cylinder transition; lower points indicate pinch-off.

stable configuration can be rendered unstable. This behavior was demonstrated experimentally. Unfortunately it is not possible to compare theory and experiment for leaky dielectrics since the requisite theory for pinned cylinders has not been developed.

ELECTROHYDRODYNAMICS OF SUSPENSIONS

Aqueous Suspensions

Until this point, attention has centered on EHD phenomena in systems with sharp interfaces. Nevertheless, the summary equations in the "Balance Laws" section clearly indicate EHD effects are possible when there is a volumetric distribution of charge or smooth variations in the dielectric constant. Do experiments support this view and to what extent do theory and experiment agree?

In a noteworthy study, Rhodes et al (1989) demonstrated EHD effects with a dilute aqueous suspension. Weak, 20-V/cm, 100-kHz fields were used to avoid electrophoresis and electro-osmosis, which are proportional to the applied field. High frequencies also rendered the effective dielectric constant of the suspension close to that of the electrolyte. The experiment was carried out as follows: First, flow of an electrolyte solution (the buffer) was established in a rectangular duct with electrodes in the sidewalls. Then, flow of a thin jet of a polystyrene latex suspension was initiated, and a continuous filament of suspension was carried through the electrode region by the buffer flow. When the conductivity of the sample exceeded that of the electrolyte solution, the suspension filament was stretched in the direction of the (oscillating) field, taking on an elliptical cross section. Since the interface was diffuse, the absence of interfacial tension as a restoring force allowed the cross section to deform continuously. In contrast, when the conductivity of the filament was lower than the surrounding solution, deformation was transverse to the applied field. The main EHD force appears to arise from free charge in the bulk induced by the applied field. Such behavior is precisely what would be expected from the leaky dielectric model, and Rhodes et al analyzed a cylindrical cross section with a sharp interface analogous to Taylor's (1966) treatment of a drop. Their discriminating function for the cylinder is

$$\Phi = R^2 + R + 1 - 3S. \tag{49}$$

At the conditions of the experiment, 100 kHz, the dielectric constant of the suspension is close to that of the electrolyte, so $S \approx 1$. Accordingly, for $R > 1$ the deformation should be prolate, and for $R < 1$, oblate, in agreement with the experimental results.

The Rhodes et al (1989) treatment lumps all the electrical forces into effects at a sharp interface. To investigate the behavior of a diffuse transition, the model equations (see "Summary Equations" section) were solved with a gradual transition in the distribution of dielectric constant and conductivity (Saville 1993). Induced charge effects were suppressed to show that field changes due to variations in conductivity combined with the $\nabla\varepsilon$-body force produce deformations analogous to those predicted by the Rhodes et al treatment. Thus, similar deformations arise from either free charge or polarization forces.

Apolar Liquid Suspensions

Following the discovery of EHD effects in aqueous suspension, similar effects were demonstrated in nonaqueous systems (Trau et al 1995a,b). Here the conductivity of a suspension of barium titanate in castor oil was adjusted using a soluble organic salt. When the conductivity of a spherical bolus of the suspension exceeded that of the surrounding castor oil, deformation was in the direction of the field; upon reversing the conductivity contrast, the bolus deformed transversely. Of course with nonaqueous systems the field strengths are high compared with those of aqueous systems. Figure 7 shows two examples of the behavior of barium titanate suspensions. Since the free charge is nil in these dispersions in the absence of a field, the theory for a diffuse transition can be used to explore the effects of induced charge ($\rho^e\mathbf{E}$-forces) and dielectric constant variation ($\nabla\varepsilon$-forces). The results agree with the predictions of the discriminating function when the transition region is thin; departures are found for thick zones. Figure 8 depicts the streamlines for a sample whose conductivity and dielectric constant are larger than the surrounding fluid. Note that all the EHD stresses are confined to the transition region. Of course the theory in this form takes no account of deformation and must be regarded as furnishing a purely qualitative picture of the initial stages of flow.

In these experiments the major electric body force appears to be derived from induced charge. To test this hypothesis, experiments were conducted without a suspension by using a dilute dye to mark the region of altered conductivity. The sense of the deformation agreed with the theory: High conductivity regions became prolate; low conductivity regions became oblate. If the conductivities of the two regions matched, then the dye did not deform when the field was applied. One would hope to do the same sort of experiment with a dielectric constant contrast but matched conductivities. This type of study has not been conducted because of the way nonconducting particles themselves alter the conductivity of a suspension. To match conductivities, a precise amount of organic electrolyte must be used, and a perfect conductivity match remains to be achieved.

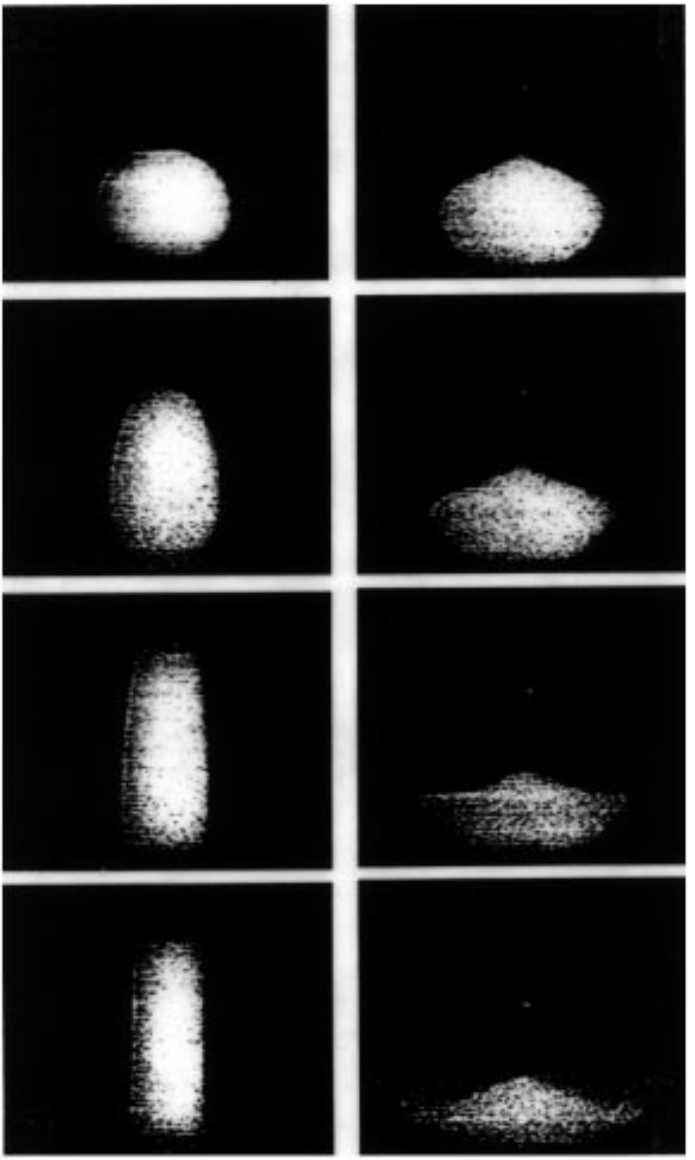

Figure 7 The behavior of barium titanate suspensions with different conductivities. The suspension on the left has a higher conductivity than the suspending fluid; on the right the conductivity is lower. In each case the field is vertical (Trau et al 1995a). Time increases from top to bottom.

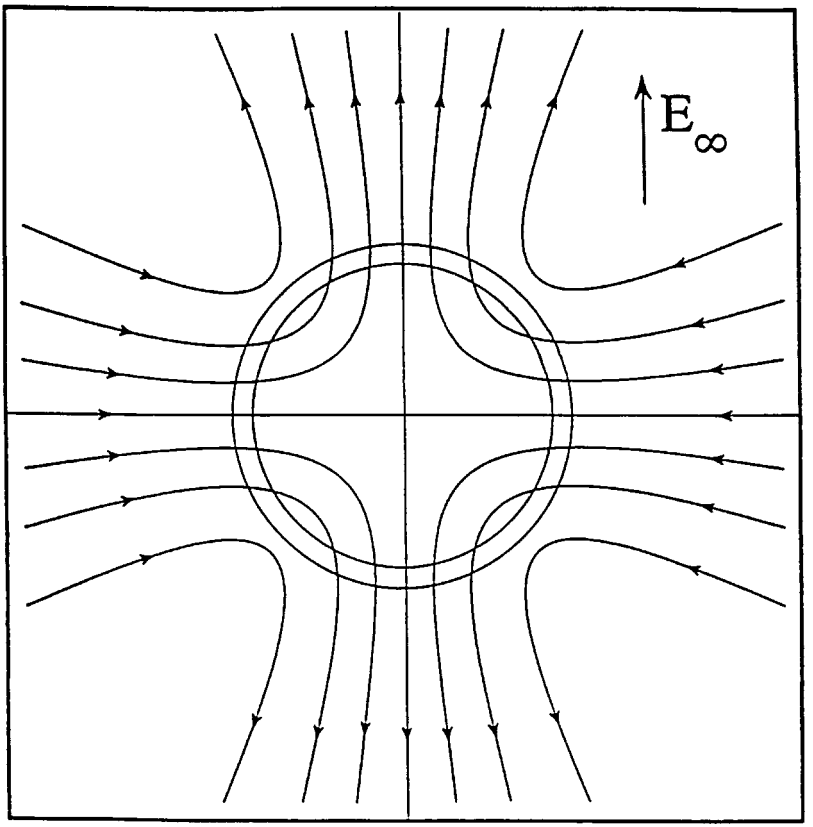

Figure 8 Flow patterns due to induced free charge and dielectric constant variations in a thin transition region (Trau et al 1995a).

CONCLUDING REMARKS

The development of the leaky dielectric model formed an important step in the construction of a unified treatment of electrohydrodynamics. The model encompasses a wide range of phenomena in polar as well as apolar liquids. As noted earlier, the leaky dielectric and electrokinetic models of electrohydrodynamics represent behavior in two rather separate circumstances: the former when free charge is induced by the field, the latter when it is an intrinsic property of an interface. In either case, it is the interaction of charge with the applied field that produces dynamical effects. Both sorts of behavior are encompassed by the same fundamental theory, with simplifications appropriate to the circumstances at hand. Insofar as the behavior of poor conductors is concerned,

Taylor's recognition of the pivotal role of charge transport and Melcher's incisive use of the model were truly significant steps. Their contributions to the development of the model justify referring to it as the Taylor-Melcher model.

Although the Taylor-Melcher model involves approximations at several levels, it finds support in most of the experimental studies to date. Certainly its qualitative predictions are in full accord with the experimental data. However, there is much to be gained from further efforts to test the theory, to uncover new phenomena and establish boundaries on its applicability. Studies of liquid bridges of the sort inaugurated by Gonzalez et al (1989), in which oscillatory fields are used to probe charge relaxation processes, are particularly promising.

ACKNOWLEDGMENTS

NASA's Microgravity Science and Applications Division has provided support for my recent work on electrohydrodynamics. I am indebted to Drs. Basaran, Castellanos, and Mestel for providing compilations of their work, along with copies of unpublished manuscripts.

Literature Cited

Ajayi OO. 1978. A note on Taylor's electrohydrodynamic theory. *Proc. R. Soc. A* 364:499–507

Allan RS, Mason SG. 1962. Particle behavior in shear and electric fields. I. Deformation and burst of fluid drops. *Proc. R. Soc. A* 267:45–61

Arp PA, Foister RT, Mason SG. 1980. Some electrohydrodynamic effects in fluid suspensions. *Adv. Colloid Interface Sci.* 12:295–356

Atten P, Castellanos A. 1995. Injection induced electrohydrodynamic flows. In *Handbook of Electrostatic Processes*, ed. AJ Kelley, JM Crowley, pp. 121–46. New York: Dekker

Bailey AG. 1988. *Electrostatic Spraying of Liquids*. New York: Wiley. 197 pp.

Basaran OA, Patzek TW, Benner RE, Scriven LE. 1995. Nonlinear oscillation and breakup of conducting, inviscid drops in an externally applied electric field. *IEC Res.* 34:3454–65

Bassett EB. 1894. Waves and jets in a viscous liquid. *Am. J. Math.* 16:93–110

Baygents JC, Saville DA. 1989. The circulation produced in a drop by an electric field: a high field strength electrokinetic model. In *Drops & Bubbles, Third International Colloquium, Monterey 1988. AIP Conference Proceedings*, ed. T Wang, pp. 7–17. New York: Am. Inst. Physics

Brazier-Smith PR. 1971. Stability and shape of isolated and pairs of water drops in an electric field. *Phys. Fluids* 14:1–6

Castellanos A. 1994. Electrohydrodynamics: basic equations and dimensionless numbers. In *Fluid Physics, Lecture Notes of Summer Schools*, ed. MG Velarde, Cl Christov, pp. 14–32. Madrid: World Scientific

Chang JS. 1987. EHD chemical reactors: a critical review. *IEEE, Industry Applications Soc. Annu. Meet. Conf. Record*, pp. 1471–79 New York: IEEE

Cloupeau M, Prunet-Foch B. 1990. Electrostatic spraying of liquids: main functioning modes. *J. Electrostat.* 25:165–84

Crowley JM. 1986. *Fundamentals of Applied Electrostatics*. New York: Wiley. 255 pp.

Debye P. 1942. Reaction rates in ionic solutions. *Trans. Electrochem. Soc.* 82:262–72

Fernandez de la Mora J, Loscertales IG. 1994. The current emitted by highly conducting Taylor cones. *J. Fluid Mech.* 260:155–84

Feynman RP, Leighton RB, Sands M. 1964. *The Feynman Lectures on Physics*, Vol. 2. Palo

Alto, CA: Addison Wesley
Fish BR. 1972. Electrical generation of natural aerosols from vegetation. *Science* 175:1239–40
Fouss RM. 1958. Ionic association. III. The equilibrium between ion pairs and free ions. *J. Am. Chem. Soc.* 80:5059–61
Gonzalez H, Castellanos A. 1993. The effect of residual axial gravity on the stability of liquid columns subjected to electric fields. *J. Fluid Mech.* 249:185–206
Gonzalez H, McCluskey FMJ, Castellanos A, Barrero A. 1989. Stabilization of dielectric liquid bridges by electric fields in the absence of gravity. *J. Fluid Mech.* 206:545–61
Hart JE, Glatzmaier GA, Toomre J. 1986. Space-laboratory and numerical simulations of thermal convection in a rotating hemispherical shell with radial gravity. *J. Fluid Mech.* 173:519–44
Hayati I. 1992. Eddies inside a liquid cone stressed by interfacial shear. *Colloids Surfaces* 65:77–84
Hayati I, Bailey Al, Tadros TF. 1986. Mechanism of stable jet formation in electrohydrodynamic atomization. *Nature* 319:41–43
Hayati I, Bailey Al, Tadros TF. 1987a. Investigations into the mechanism of electrohydrodynamic spraying of liquids I. *J. Colloid Interface Sci.* 117:205–21
Hayati I, Bailey Al, Tadros TF. 1987b. Investigations into the mechanism of electrohydrodynamic spraying of liquids. II. *J. Colloid Interface Sci.* 117:222–30
Huebner AL. 1969. Disintegration of charged liquid jets. *J. Fluid Mech.* 38:679–88
Hurle DTJ, Muller G, Nitsche R. 1987. *Crystal Growth from the Melt in Fluid Science and Materials Science in Space: A European Perspective*, ed. HU Walter, CH. X, New York: Springer Verlag. 743 pp.
Kang IS. 1993. Dynamics of a conducting drop in a time-periodic electric field *J. Fluid Mech.* 257:229–64
Landau LD, Lifshitz EM. 1960. *Electrodynamics of Continuous Media*. Oxford: Pergamon. 417 pp.
Melcher JR. 1972. Electrohydrodynamics. In *Proc. 13th Int. Congr. Theoret. Appl. Mech.* (*Moscow*), ed. E Becker, GK Mikheilov, pp. 240–63. Berlin: Springer Verlag
Melcher JR. 1981. *Continuum Electromechanics*. Cambridge, MA: MIT Press
Melcher JR, Schwartz WJ. 1968. Interfacial relaxation overstability in a tangential electric field. *Phys. Fluids* 11:2604–16
Melcher JR, Taylor GI. 1969. Electrohydrodynamics: a review of the role of interfacial shear stresses. *Annu. Rev. Fluid Mech.* 1:111–46
Mestel AJ. 1994. Electrohydrodynamic stability of a slightly viscous jet. *J. Fluid Mech.* 274:93–113
Mestel AJ. 1996. Electrohydrodynamic stability of a highly viscous jet. *J. Fluid Mech.* 312:311–26
Moelwyn-Hughes, EA. 1965. *Physical Chemistry*. Oxford: Pergamon. 1334 pp.
Nayyar NK, Murthy GS. 1960. The stability of a dielectric liquid jet in the presence of a longitudinal electric field. *Proc. Phys. Soc.* 75:369–73
O'Konski CT, Thacher HC Jr. 1953. The distortion of aerosol droplets by an electric field. *J. Phys. Chem.* 57:955–58
Pelekasis NA, Tsamopoulos JA, Manolis GD. 1990. Equilibrium shapes and stability of charged and conducting drops. *Phys. Fluids A* 2:1328–40
Ptasinski KJ, Kerkhof PJAM. 1992. Electric field driven separations: phenomena and applications. *Separation Sci. Technol.* 27(8/9):995–1021
Raco RJ. 1968. Electrostatically supported column of liquid. *Science* 160:311–12
Ramos A, Castellanos A. 1994a. Conical points in liquid-liquid interfaces subjected to electric fields. *Physics Lett. A* 184:268–72
Ramos A, Castellanos A. 1994b. Equilibrium shapes and bifurcation of captive dielectric drops subjected to electric fields *J. Electrostat.* 33:61–86
Ramos A, Gonzalez H, Castellanos A. 1994. Experiments on dielectric liquid bridges subjected to axial electric fields *Phys. Fluids* 6:3206–8
Rayleigh, Lord. 1882. On the equilibrium of liquid conducting masses charged with electricity. *Phil. Mag. Ser.* 5. 14:184–86
Rayleigh, Lord. 1945. *The Theory of Sound*, Vol. 2. New York: Dover. 504 pp.
Rhodes PH, Snyder RS, Roberts GO. 1989. Electrohydrodynamic distortion of sample streams in continuous flow electrophoresis. *J. Colloid Interface Sci.* 129:78–90
Russel WB, Saville DA, Schowalter WR. 1989. *Colloidal Dispersions*. Cambridge, UK: Cambridge Univ. Press. 525 pp.
Sankaran S, Saville DA. 1993. Experiments on the stabilty of a liquid bridge in an axial electric field. *Phys. Fluids A* 5:1081–83
Saville DA. 1970. Electrohydrodynamic stability: fluid cylinders in longitudinal electric fields. *Phys. Fluids* 13:2987–94
Saville DA. 1971a. Stability of electrically charged viscous cylinders. *Phys. Fluids* 14:1095–99
Saville DA. 1971b. Electrohydrodynamic stability: effects of charge relaxation at the interface of a liquid jet. *J. Fluid Mech.* 48:815–27
Saville DA. 1974. Electrohydrodynamic oscillation and stability of a charged drop. *Phys.*

Fluids 17:54–60
Saville DA. 1977. Electrokinetic effects with small particles. *Annu. Rev. Fluid Mech.* 9:321–37
Saville DA. 1993. Electrohydrodynamic deformation of a particulate stream by a transverse electric field. *Phys. Rev. Lett.* 71:2907–10
Scott TC. 1989. Use of electric fields in solvent extraction: a review and prospectus. *Separation Purification Meth.* 18(1):65–109
Sherwood JD. 1988. Breakup of fluid droplets in electric and magnetic fields. *J. Fluid Mech.* 188:133–46
Sherwood JD. 1991. The deformation of a fluid drop in an electric field: a slender body analysis. *J. Phys. A: Math. Gen.* 24:4047–53
Sozou C. 1972. Electrohydrodynamics of a liquid drop: the time dependent problem. *Proc. R. Soc. A* 331:263–72
Spertell RB, Saville DA. 1976. The role of electrohydrodynamic phenomena in the motion of drops and bubbles. In *Proc. Int. Colloq. Drops Bubbles*, ed. M Plesset, 1:106–19. Pasadena: Calif. Inst. Technol.
Taylor GI. 1964. Disintegration of water drops in an electric field. *Proc. R. Soc. A* 280:383–97
Taylor GI. 1966. Studies in electrohydrodynamics I. The circulation produced in a drop by an electric field. *Proc. R. Soc. A* 291:159–66
Taylor GI. 1969. Electrically driven jets *Proc. R. Soc. A* 313:453–75
Tobazeon R. 1984. Electrohydrodynamic instabilities and electroconvection in the transient and a.c. regime of unipolar injection in insulating liquids: a review. *J. Electrostat.* 15:359–84
Torza S, Cox RG, Mason SG. 1971. Electrohydrodynamic deformation and burst of liquid drops. *Phil. Trans. R. Soc. A* 269:295–319
Trau M, Sankaran S, Saville DA, Aksay IA. 1995a. Electric-field-induced pattern formation in colloidal dispersions. *Nature* 374:437–39
Trau M, Sankaran S, Saville DA, Aksay IA. 1995b. Pattern formation in non-aqueous colloidal dispersions via electrohydrodynamic flow. *Langmuir* 11:4665–72
Tsukada T, Katayama T, Ito Y, Hozawa M. 1993. Theoretical and experimental studies of circulations inside and outside a deformed drop under a uniform field *J. Chem. Eng. Jpn.* 26:698–703
Vizika O, Saville DA. 1992. The electrohydrodynamic deformation of drops suspended in liquids in steady and oscillatory fields. *J. Fluid Mech.* 239:1–21
Wohlhuter FK, Basaran O. 1992. Shape and stability of pendant and sessile dielectric drops in an electric field. *J. Fluid Mech.* 235:481–510